Impact of mass ratio and surface roughness on vortex induced vibrations

Author

Muhammad Usman Anwar

Regn Number

00000277916

Supervisor

Dr. Niaz Bahadur Khan

DEPARTMENT OF DESIGN AND MUFACTURING ENGINEERING

SCHOOL OF MECHANICAL & MANUFACTURING ENGINEERING

NATIONAL UNIVERSITY OF SCIENCES AND TECHNOLOGY

ISLAMABAD

March, 2021

Impact of mass ratio and surface roughness on vortex induced vibrations

Author

Muhammad Usman Anwar

Regn Number

00000277916

A thesis submitted in partial fulfillment of the requirements for the degree of

MS Design and Manufacturing Engineering

Thesis Supervisor:

Dr. Niaz Bahadur Khan

Thesis Supervisor's Signature: _____

DEPARTMENT OF DESIGN AND MUFACTURING ENGINEERING

SCHOOL OF MECHANICAL & MANUFACTURING ENGINEERING

NATIONAL UNIVERSITY OF SCIENCES AND TECHNOLOGY,

ISLAMABAD

March, 2021

THESIS ACCEPTANCE CERTIFICATE

Certified that final copy of MS/MPhil thesis Written by Mr. Muhammad Usman Anwar (Registration No: 00000277916), of SMME (School of Mechanical and Manufacturing Engineering) has been vetted by undersigned, found complete is all respects as per NUST Statutes/ Regulations, is free of plagiarism, errors and mistakes and is accepted as partial fulfillment for award of MS/MPhil Degree. It is further certified that necessary amendments as pointed out by GEC members have also been incorporated in this dissertation.

Signature: _____

Name of the supervisor: Dr. Niaz Bahadur Khan

Dated: _____

Signature (HOD): _____

Dated: _____

Signature (Principal): _____

Dated: _____

MASTER THESIS WORK

We hereby recommend that the dissertation prepared under our supervision by: Muhammad Usman Anwar 00000277916 Titled: "Impact of mass ratio and surface roughness on vortex induced vibrations" be accepted in partial fulfillment of the requirements for the award of MS Design and Manufacturing Engineering degree with (…….) grade.

Examination Committee Members

1. Name: Dr. Mian Ashfaq Ali Signature: _____

2. Name: Dr. Emad ud Din Signature: _____

3. Name: Dr. Najam ul Qadir Signature: _____

Supervisor's name: Dr. Niaz Bahadur Khan Signature: _____

Date: _____

_____ Date: _____

Head of Department

COUNTERSIGNED

_____ Date: _____

Dean/principal

Declaration

I certify that this research work titled “Impact of mass ratio and surface roughness on vortex induced vibrations” is my own work. The work has not been presented elsewhere for assessment. The material that has been used from other sources. It has been properly acknowledged / referred.

Signature of Student

Muhammad Usman Anwar

2018-NUST-MS-DME-00000277916

Plagiarism certificate (Turnitin Report)

This thesis has been checked for Plagiarism. Turnitin report endorsed by Supervisor is attached.

Signature of Student

Muhammad Usman Anwar

2018-NUST-MS-DME-00000277916

Signature of the supervisor

Copyright statement

- Copyright in text of this thesis rests with the student author. Copies (by any process) either in full, or of extracts, may be made only in accordance with instructions given by the author and lodged in the Library of NUST School of Mechanical & Manufacturing Engineering (SMME). Details may be obtained by the Librarian. This page must form part of any such copies made. Further copies (by any process) may not be made without the permission (in writing) of the author.
- The ownership of any intellectual property rights which may be described in this thesis is vested in NUST School of Mechanical & Manufacturing Engineering, subject to any prior agreement to the contrary, and may not be made available for use by third parties without the written permission of the SMME, which will prescribe the terms and conditions of any such agreement.
- Further information on the conditions under which disclosures and exploitation may take place is available from the Library of NUST School of Mechanical & Manufacturing Engineering, Islamabad

Acknowledgement

I am thankful to my Creator Allah Subhana-Watala to have guided me throughout this work at every step and for every new thought which You setup in my mind to improve it. Indeed I could have done nothing without your priceless help and guidance. Whosoever helped me throughout the course of my thesis, whether my parents or any other individual was your will, so indeed none be worthy of praise but you.

I am profusely thankful to my beloved parents who raised me when I was not capable of walking and continued to support me throughout in every department of my life. Especially my father who is the real boss of my life. He has planned my life quite efficiently and teaches me to do hard work whatever the circumstances are.

I would also like to express special thanks to my supervisor Dr. Niaz Bahadur khan for his help throughout my thesis and also for the motivation and determination he gave me. He cares so much about any of his student's work and responds to queries and question so promptly.

I would also like to pay special thanks to Dr. Emad ud din for his tremendous support and cooperation. Each time I got stuck in something, he came up with the solution. Without his help I wouldn't have been able to complete my thesis. I appreciate his patience and guidance throughout the whole thesis.

I would also like to thank Mr. Najam ul Qadir and Mr. Mian Ashfaq Ali for being on my thesis guidance.

Finally, I would like to express my gratitude to all the individuals who have rendered valuable assistance to my study.

Dedicated to my exceptional parents and adored siblings whose tremendous support and cooperation led me to this wonderful accomplishment.

Abstract

Fluid structure interactions have been thoroughly studied in the past few decades due to their high importance in engineering applications. This phenomenon plays an important role for example in offshore risers, high slender buildings, chimney stacks, heat exchangers, etc. The vortices shedding from the bluff body can induce high-amplitude oscillations. This phenomenon is known as vortex-induced vibrations (VIV). In this thesis, a numerical study has been performed to better understand the impact of mass ratio and surface roughness on vortex induced vibrations. The work concentrates on vortex induced vibration in a 2D circular cylinder having different mass ratios and surface roughness at a high Reynolds Number (Re) = 10^4. The cylinder was elastically mounted on a mass-spring-damper system, with 1 degree of freedom (dof). The numerical solution is calculated using Reynolds-averaged Navier–Stokes (RANS) equations with computational fluid dynamic (CFD) tools. All the calculations were performed with kw-sst model. The study results concluded that VIV phenomenon is strongly affected by the mass ratio and surface roughness. Higher mass ratios result in shortening of lock-in region with a decrease in amplitude response. It was concluded from the study that rough cylinders have smaller amplitude response and a narrower lock-in region as compared to smooth cylinders. Vortex modes of 2S, 2P, P+S and 2T were observed in this study which agree well with the amplitude response.

Keywords: Flow induced vibrations, reduced velocity, surface roughness, mass ratio

Table of Contents

List of Figures

List of Tables

Chapter 1: Introduction

1.1 Background

Fluid flow over rigid bodies is such a common phenomenon, that it can be encountered in almost every aspect of our worldly experience. This fluid structure interaction is of great importance, as the fluid flowing past the structure can induce VIV phenomenon. Vortex induced vibrations can be extremely destructive in nature, they affect many engineering applications such as skyscrapers, power transmission lines, underwater pipelines and bridge decks. Offshore industry is one of the most vulnerable fields to VIV due to the extensive constructions in flowing water. Drilling risers, catenaries, marine cables and underwater pipelines are a few examples that are highly susceptible to Vortex induced vibrations. A cylinder undergoing vortex induced vibrations can be seen in figure 1.

VIV phenomenon is highly dependent on the physical properties (such as mass, shape and condition of the surface) of the bluff body. Surface roughness plays an important role in physical and chemical phenomena and is, therefore, of great importance in science and engineering. Flow past a bluff body with some degree of surface roughness behaves differently in comparison to that of a smooth body. Thus, affecting the flow characteristics and VIV phenomenon. In real life every surface is rough up to some extent. In addition to surface roughness, mass ratio has significant impact on the flow characteristics and vortex formation.

The purpose of the study is to validate the available experimental data and build the confidence on numerical analysis to reduce the cost of studying the VIV phenomenon. The study will result in better understanding of the impact of surface roughness and mass ratio on the VIV phenomenon and flow characteristics.

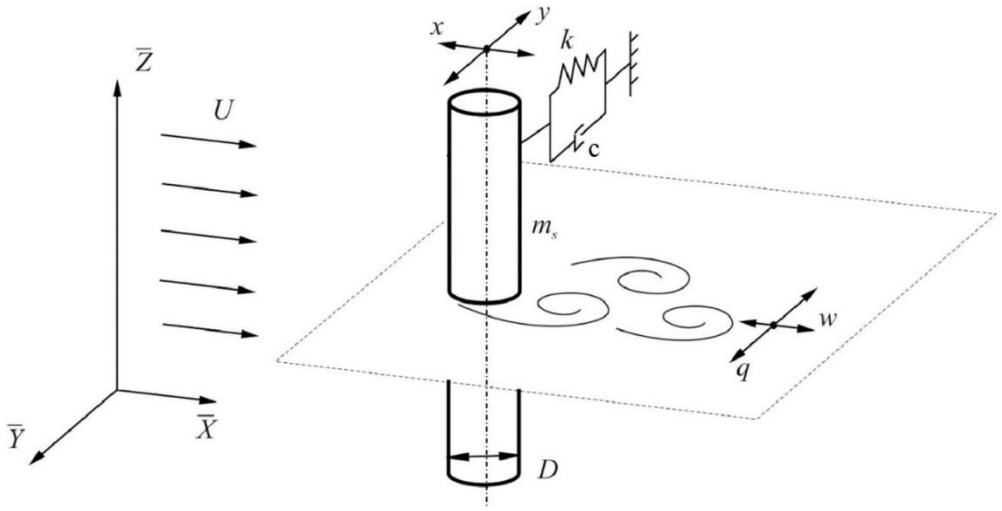

Figure 1. Schematic diagram of a cylinder undergoing VIV

1.2 Literature Review

Feng [1] in 1969 conducted experimental works to develop understanding of VIV phenomenon in terms of the response amplitude, phase angle, wake velocity and frequencies for varying reduced velocities and levels of damping. Feng's work covered the 'lock-in' region, where vortex shedding frequency becomes equal or close to the natural frequency of the body. Lock-in region is an area of major interest as amplitude response reaches maximum value. Blevins [2] conducted a study to find that the vortex shedding happening around the cylinder generates time-dependent drag and lift forces over a certain Reynolds number range. In case of a flexibly mounted cylinder these forces can induce vibrations in the cylinder. The lift induces cross-flow (CF) vibrations, and the drag induces inline (IL) vibration, combination of CF vibrations and IL vibrations is known as vortex-induced vibration (VIV). Breuer [3], Sarpkaya [4] and Bearman [5] performed extensive study and has cleared many ambiguities regarding the restrictions faced during numerical solutions. Breuer [3] performed a numerical study at Re=3900 using large eddy simulation (LES) for flow past a circular cylinder. The results show good agreement with experimental data. The reviews conducted by Sarpkaya [4] and Bearman [5] elucidated that amplitude response is highly susceptible to Reynolds number which is well documented at low Reynolds numbers more research is required to understand its effect at high subcritical values and

through the critical range since many practical applications are found in these flow regimes. Large-eddy simulation, Reynolds averaged NS and Direct-numerical simulations are mainly used in case of turbulent flow. RANS is emerging technique due to its low computational cost and acceptable results. Studies on VIV in circular cylinders at higher Reynolds Number are still scarce whereas low Re and low mass ratios have been covered many times in numerous studies. Placzek et al. [6] performed a numerical study using 2D (2 Dimensional) RANS code to investigate VIV phenomenon at low mass ratio and low Reynolds number (RE=100). The vortex shedding mode was effectively captured by 2D RANS code at low RE (RE = 100).

By utilizing 3-dimensional Navier-Stokes equations Zhao et al. [7] studied the VIV in Re range of Re =150 to 1000. From these studies it was realized that 2D Navier-Stokes are not suitable for the solution VIV in turbulent flows. On the other hand, using 2D (2 Dimensional) Rans code gave reliable results. Niaz et.al [8] performed a study at Re = 3900 around a fixed structure using LES code along the Smagorinksy—Lilly subgrid-scale model to develop a better understanding of the impact of spanwise length and mesh resolution on calculating recirculation length and angle of separation. Khalak and Williamson [9] performed experimental studies at low mass ratio in the Reynolds number range of Re = 1,700 to 12,000 for the comprehension of VIV phenomenon. Guilmineau and Queutey [10], Pan and Cui [11] and Wei Li et al. [12] conducted numerical studies to validate their results with expermintal results obtained by Khalak and Williamson [9] but despite predicting the vortex-shedding mode and the transition among different modes, their studies couldn't compute the maximum amplitude response. Nguyen V-T and Nguyen HH [13] performed a study by using detached-eddy simulation (DES) [which is hybrid of RANS and LES] at low mass ratio and high Reynolds number, to validate their results with experimental work done by Hover [14]. And it did show good agreeability with experimental results. Niaz et.al [15] performed a numerical study using computationally less expensive RANS shear–stress-transport (SST) k-w turbulent model at high Reynolds number (10^4) and low mass ratio, the results agreed well with the experimental studies and 3-dimensional DES.

Mass ratio of a bluff body is an important parameter, which significantly affects the flow characteristics and VIV phenomenon. In a review study by Williamson and Govardhan [32], a thorough analysis was performed on the effect of mass and damping ratios. Their review showed that how mass ratio influences, the dominant frequency in synchronization conditions, the maximum amplitude response in upper and lower branches, and the upper limit of Ur of the synchronization region. B. Stappenbelt et al. [22] conducted a physical experiment to find out that with decreasing mass ratio lock-in region

widened and traverse amplitude response increased. Bahmani and Akbari [39] analyzed the effect of mass and damping ratios via 2D simulations in the laminar regime with Reynolds number ranging from 80 to 160 and the mass ratios are m*=74.5, 149, 298. They found that the results agreed well with the literature, increase in m*ζ (by either varying m* or ζ) decreased the maximum amplitude response and the reduced velocity range over which lock-in occurs. Alireza modir et al. [23] performed an experimental study for an elastically mounted rigid circular cylinder within Reynolds numbers (1.7 x 104 < Re < 7 x 104) in a high damping system for mass ratios of (m* = 1.6, 2.3 and 3.4) and concluded that the maximum amplitude of oscillation and the range of synchronization strongly depend on mass ratio. As m* decreases, the maximum VIV response increases and the synchronization range widens and shifts towards the higher Reynolds numbers.

Pigazzini, R. et al. [38] conducted a study on an elastically mounted circular cylinder by using URANS code at Reynolds number in order of 10^4 for three different mass ratios (m∗=1.2, 2.4, 3.6) to investigate the effect of mass ratio on VIV response of 1DOF multi-frequency cylinder system in traverse direction. The study gave a profound insight into the characteristics of vortex-induced lift force. For specific combinations of (Ur, m∗), ultra- and sub-harmonic terms are observed to take the control of the VIV process, both at lock-in and in desynchronization regions. This study focused only on limited number of mass ratios and 1DOF vibrating system. J. Zhao et al. [37] conducted an experimental study for an elastically mounted square cylinder in the Reynolds number range of 1000<Re<12300 to investigate the effect of mass ratio (ranging from m*=2.64 to 15) on the crossflow VIV response for three angles of attack, α= 0º, 20º and 45º. It was found that at α= 0º the VIV galloping response decreased with an increase in mass ratio, for m* ≥ 11.31 it completely diminished. For α= 45º, there was only marginal reduction in the peak response & for α= 20º, after critical mass ratio m*=3.5 there were no higher branch subharmonic VIV. Z. Tang et al. [40] analyzed the effect of spring stiffness and mass ratio ($2 \leq m^* \leq 10$) on flow-induced vibration (FIV) of a square cylinder placed at four different incidence angles, α= 0º, 10º, 22.5º and 45º. The results showed that a critical mass ratio exists (m^*_{crit}=2.8) below which galloping disappears. Chen et al. [41] analyzed the VIV response of a circular cylinder with low mass ratio (m*=2.39) and moderate Reynolds numbers (within the range 1155 through 6934) through a nonlinear energy sink (NES) using RANS code and kw-SST model. The results showed that placing NES inside of the low mass ratio cylinder affected the distribution of three branches, narrowed the lock-in region and shifted it towards left.

Various studies have been conducted to study the effects of surface roughness on vortex induced vibrations of a circular cylinder as shown in Table 1, Okajima et al. [16] performed a study of a flexible cylinder in air whereas Allen & Henning [17]; Bernitsas et al. [18]; Kiu et al. [19]; Gao et al. [20]), performed studies of flexible cylinders in water. Okajima et al. [16] performed a study in the subcritical Reynolds number range and the amplitude response of a rough cylinder is smaller in comparison to a smooth cylinder. Whereas, VIV amplitude of the rough cylinder is higher in comparison to a smooth cylinder, in the critical Reynolds number range. At present, there are many experimental studies on the rough cylinder in the air, but few on the characteristics of the rough cylinder in the water. Allen & Henning [17] performed a study within the critical and supercritical Reynolds number to investigate the effects of surface roughness on the cylinder VIV. There was no significant effect on the VIV response due to the surface roughness. Which is due to the fact that smooth cylinder has low resistance in the critical range and the smooth cylinder has no amplitude response.

Bernitasas et al. [18] performed an experimental study in the range of $8 \times 10^3 < Re < 2.0 \times 10^5$ to investigate the VIV phenomenon of an elastically mounted circular cylinder with rough bands. The study concluded that the flow characteristics of the fluid near the cylinder are highly sensitive to the roughness grit size, width and location of the rough bands. The study showed that roughness magnitude and distribution can be utilized to control or maneuver the VIV response and the range of lock-in region. Kiu et al. (19) performed an experimental study in the range of 1.7×10^4 to 8.3×10^4 on an elastically mounted rigid cylinder and found that with the increasing roughness, the maximum VIV amplitude and the mean drag coefficient decrease, tending toward constant values. The Strouhal numbers of rough cylinders are higher in comparison to smooth cylinders. Gao et al. [20] designed a physical experiment method to study the influence of surface roughness on VIV response of a riser, and compared the resistance, lift force, tension, vortex shedding frequency, vibration frequency and displacement response of the risers with different surface roughness.

The VIV lock-in phenomenon occurs earlier in the streamwise direction in comparison to transverse direction, so the VIV amplitude response is higher for streamwise direction as compared to transverse direction at the low reduced velocities. The rough riser had a smaller VIV amplitude response, higher vortex shedding frequency and a narrower “Lock-in” region, in comparison to that of smooth riser. Y. Gao et al. [21] performed a study with 2D RANS approach and a SST k–ω turbulence model at RE=5000 for a smooth cylinder and a rough cylinder with different degrees of roughness, and found that reduced velocity could be divided into four parts: initial branch, upper branch, lower branch and

desynchronization region based on the VIV. Rough cylinders have smaller VIV response and lock-in region compared to smooth cylinders.

N A S Ramzi et al [33] performed an experimental study on a short rigid cylinder to investigate VIV phenomenon and dynamic responses in cross-flow direction at different surface roughness. The experimental study was performed in the range of 1m/s to 8m/s of wind speed, the experimental setup used an accelerometer and LMS TestXpress software for recording and processing of amplitude response readings respectively. The study found that the higher surface roughness resulted in higher amplitude response reductions. Mohd Kushairi Mohd Ghazali et al. [34] performed an experimental study in subcritical range of Reynolds number from 4.9 × 10^3 to 1.5 × 10^4 for a cylinder with roughness coefficient varying from 0.19 × 10^-3 to 5.10 × 10^-3. The study found that as the surface roughness increases the amplitude response of the structure decreases, due to the formation of narrow wake regions. In addition to this, the frequency of the vibration also increased with an increase in surface roughness whereas amplitude response was found to be small. Y. Gao et al. [35] performed a numerical study at RE=5000 with 2D URANS and SST k−ω turbulence model for rough oscillating cylinder in the vicinity of a plane wall. On the basis of amplitude response in cross-flow direction, the reduced velocity range can be divided into three regions; pre-lock-in, lock-in, and post-lock-in. The results showed that the VIV trajectory of the cylinder is highly sensitive to the reduced velocity but not to the surface roughness. Cylinder with initial small gap displayed a coalescing effect with formation of weak 2S vortex mode, while there was no coalescing effect for cylinder with large initial gap and asymmetric 2S vortex mode was found in the wake region.

X. Han et al. [36] performed a numerical study for a 2DOF vibrating cylinder system in the Reynolds number range of 1500 to 10500 with 2D RANS and SST k−ω turbulence model for varying surface roughness. It was found that the rough cylinder VIV also has SS branch, AS branch, initial branch, super upper branch and lower branch. The rough cylinder also has 2S, 2T and 2P wake vortex shedding patterns just like smooth cylinders, in the range of reduced velocity Ur = 2.0–14.0. Different from smooth cylinder, rough cylinder also produces 2P wake vortex shedding pattern in the low reduced velocity range, but in the high reduced velocity range, when the surface roughness Ks/D = 0.005 and 0.01, the surface roughness of cylinder will suppress the generation of 2P wake vortex shedding pattern which changes to 2S wake vortex shedding pattern.

One of the objectives of the study is to build confidence in the RANS kw-sst model for predicting VIV phenomenon of a circular cylinder. This study was conducted on a smooth cylinder (Ks/D = 0, where

Ks is the diameter of a hypothetical grain of sand) and on a rough cylinder with roughness value (i.e., Ks/ D = 2 × 10−2) with mass ratios of 2.4 and 11. For each surface roughness and mass ratio, 6 different reduced velocities ranged from 2 to 14 were selected for the study. Therefore, there were 24 simulation cases in total.

Table 1. Analyses of flexible cylinders having different degrees of surface roughness.

Author	**Year**	**Reynolds Number**	**Surface Roughness**
In air			
Okajima et al. [16]	1999	$2.5x10^{4} – 3.2x10^{5}$	$5x10^{-3} – 3.8\ x10^{-2}$
In water			
Allen and Henning [17]	2001	$1.8x10^{5} – 6.5x10^{5}$	$5.1x10^{-5} – 5.8\ x10^{-3}$
Bernitsas et al. [18]	2008	$8.0x10^{3} – 2.0x10^{5}$	$1.4x10^{-5} – 4.2\ x10^{-3}$
Kiu et al. [19]	2011	$1.7x10^{4} – 8.3x10^{4}$	$2.8x10^{-4} – 1.4\ x10^{-2}$
Gao et al. [20]	2015	$2.5x10^{4} – 1.8x10^{5}$	$1.1x10^{-4} – 1.2\ x10^{-2}$

Objectives:

This research work includes following objectives:

- To study the impact of mass ratio on vortex shape, crossflow amplitude and lock-in region.
- To study the impact of surface roughness on vortex shape, crossflow amplitude and lock-in region.
- To assess the capability of RANS model.

Chapter 2: Numerical approach

This chapter demonstrates the numerical approach used for a rigid cylinder undergoing vortex induced vibrations with one degree of freedom in crossflow direction. All the simulations are performed at a subcritical Reynold's Number of 10000 and will be carried out at reduced velocities in the range of $2 \leq Ur \leq 14$.

2.1 Incompressible Navier-Stokes Equations

In this current study, the fluid flow past a cylinder is considered an incompressible, two dimensional and unsteady flow. The unsteady Reynolds−Averaged–Navier-Stokes (RANS) equations can be written as:

$$\frac{\partial \overline{u_i}}{\partial x_i} = 0, \tag{1}$$

$$\frac{\partial \overline{u_i}}{\partial t} + \frac{\partial \overline{u_i u_j}}{\partial x_j} = -\frac{1}{P}\frac{\overline{\partial p}}{\partial x_i} + \nu \nabla^2 \overline{u_i} - \frac{\partial \overline{u_i' u_j'}}{\partial x_j}, \tag{2}$$

in which

$$-\overline{u_i' u_j'} = \nu_t \left(\frac{\partial u_i}{\partial x_j} + \frac{\partial u_j}{\partial x_i}\right) + \frac{2}{3}\delta_{ij} k, \tag{3}$$

where u_i and u_j represent the instantaneous velocity components in the i and j directions, respectively; for example, u and ν are velocity in the x and y directions, respectively; u_i and u_j are fluctuation velocity components in the i and j directions, respectively. Furthermore, x_i and x_j are Cartesian coordinates in the i and j directions, respectively; t is time; p is pressure; ρ and υ are the density and kinematic viscosity of fluid, respectively; υ_t is the turbulent viscosity and k is the turbulent energy.

The SST k−ω turbulence model was proposed by Menter [24] which is an improved version of the standard k−ω model combining the pros of both k-w model and k-epsilon model. In comparison to direct numerical simulation (DNS) and large eddy simulation (LES), numerical simulation using the SST k−ω model consumes much less computational cost.

2.2 Simulation model

The schematic diagram of the elastically mounted circular cylinder for 2D flow simulation in cross flow direction can be seen in Figure 2. For simulation of vibrating cylinders, the cylinder is considered as a mass-spring damping system consisting of mass (m), stiffness (K) and damping (c).

The motion generated in the cylinder in the crossflow direction as a results of acting fluid forces can be expressed mathematically as:

$$m\ddot{y} + c\dot{y} + Ky = F_y \tag{4}$$

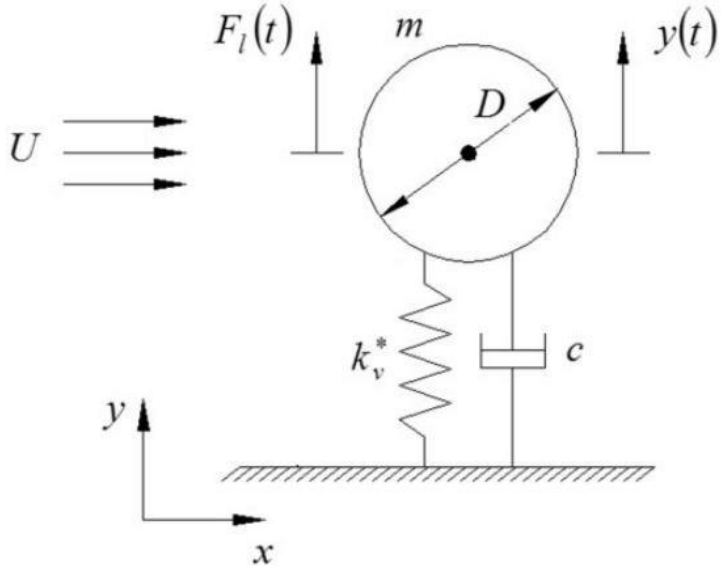

Figure 2. Schematic diagram of the elastically mounted circular cylinder in cross flow

2.3 Numerical Method for 1-DOF system

An option in ANSYS Fluent, named as Six degree of freedom method (SDOF), is utilized for the investigation of the VIV phenomenon in transverse direction. The relevant properties of the moving objects are specified using the Macro, (*DEFINE_SDOF_PROPERTIES*) for the SDOF solver in ANSYS Fluent. SDOF can be utilized for 1 degree of freedom by constraining motions in 5 other directions, by utilizing a command line in the User-Defined Function file. (Appendix)

The acceleration of the cylinder is calculated by solving all the external elastic forces acting on it. The velocity and displacement in the time domain can be calculated accordingly. The motion of the center of gravity is mathematically expressed as:

$$\dot{v_G} = \frac{1}{m}\sum f_G \tag{5}$$

where $\dot{v_G}$ is the accelration, m is the mass and f_G represents all forces acting on the body.
After applying on the rigid cylinder:

$$\ddot{y} = \frac{1}{m}\sum f_G = \frac{F_y - c\dot{y} - ky}{m} \tag{6}$$

where y, $\dot{y}$, $\ddot{y}$ are the displacement, velocity and acceleration of the cylinder at the same timestep, Fy is the fluid force and $c\dot{y}$ and ky are the elastic forces acting on the system. The position of rigid body is calculated and updated at each timestep by dynamic mesh method from velocity.

The velocity at each time step is given by:

$$\dot{y}_n = \ddot{y}_{n-1}\Delta t \tag{7}$$

2.4 Non-dimensional parameters:

All the parameters in this study are non-dimensional and are defined as below.

Mass ratio

The mass ratio of a cylinder is defined as the ratio of mass of the oscillating cylinder (m_{osc}) to the mass of fluid displaced (m_f).

It is given as

$$m^* = \frac{m_{osc}}{m_f} \tag{8}$$

Where $m_f = \frac{1}{4}\rho\pi D^2 L$

where ρ, D and L represent the density of fluid, diameter of cylinder and submerged length of cylinder, respectively.

Reynolds number (Re)

The ratio of inertial force to viscous force within the fluid is known as Reynolds number and is given by;

$$Re = \frac{UD}{\upsilon} \tag{9}$$

where U, D and υ represent the inlet velocity, characteristics length and kinematic viscosity, respectively

Reduced velocity

Reduced velocity (Ur), which is mean velocity normalized by diameter of cylinder and natural frequency of structure, is an important parameter when the structure begins oscillation due to the VIV phenomenon. This parameter is defined by

$$U_r = \frac{U}{Df_n} \tag{10}$$

Where U, D and f_n are velocity of fluid, diameter of cylinder and natural frequency of structure, respectively.

Some of the other non-dimensional terms that have been used in this study are shown in Table 2.

Table 2. Definitions of non-dimensional parameters and variables

A^*	A/D	Amplitude ratio
m_d	$\frac{\pi}{4}\rho D^2 L$	The displaced fluid mass
$m_{cylinder}$		Mass of cylinder
m_a	$C_a m_d$	Added mass
m_o	$m_a + m_{cylinder}$	Oscillating system mass
m^*	m_o/m_d	Mass ratio
f_n	$\frac{1}{2\pi}\sqrt{\frac{K}{m_{cylinder}}}$	System natural frequency
f_o		Oscillating frequency of the cylinder
f^*	$\frac{f_o}{f_n}$	Frequency ratio
U_r	$\frac{U}{f_n D}$	Reduced velocity based on natural frequency
c	$4\pi\zeta m f_n$	System damping

Chapter 3: Design & Development Methodology

3.1 Problem Statement

The aim of this project is to analyse the effect of mass ratio and surface roughness on vortex induced vibrations using ANSYS/fluent. This research work will focus on three main parameters:

- Cylinder amplitude Response
- Vortex mode
- Hydrodynamic force coefficients (Cd, Cl)

The study is divided into two sections:

Section 1: Impact of mass ratio on vortex induced vibrations

Section 2: Impact of surface roughness on vortex induced vibrations

This study was conducted on a smooth cylinder with Ks/D = 0, where Ks is the diameter of a hypothetical grain of sand) and on rough cylinders with roughness value (i.e., Ks/ D = 2 × 10−2) For both smooth and rough cylinder mass ratios of 2.4 and 11 were used. For each surface roughness and mass ratio, 6 different reduced velocities ranged from 2 to 14 were selected for the study. Therefore, there were 24 simulation cases in total. The change in Ur is achieved by changing the natural frequency of the cylinder.

3.2 Flow requirements/ Computational domain

Fluid flow is highly dependent on the size of the flow domain. In literature different domain sizes have been used.

- Shao [25] performed a numerical study using RANS code with the domain size of 30D × 16D for flow around cylinder.
- Fang and Han [26] used a domain size of 8D in traverse direction, for the numerical study of the hydrodynamic performance.
- Franke J, Frank W [27] performed a numerical study using LES model with the domain size of 25D × 20D for flow around a circular cylinder.

In many previous studies, it was observed that smaller domain size significantly effects the formation of vortices in the wake region, so, a sufficiently large domain size is preferred to avoid the disturbances caused by boundary conditions.

Zdravkovich [28], Navrose [29] and Zhao [30] concluded from their work, that 5% of the blockage ratio (which is the ratio of cylinder diameter to the domain width) is assumed to be adequate to minimize the effects of on cylinder response. Therefore, a computational domain size of 45D × 20D is used in this study which meets the criteria (Fig 2).

The inlet boundary, which is on the left side of the domain, is placed at a distance of 15D from the cylinder; the outlet boundary, which is at the right side of the cylinder, is placed at a distance of 30D from the cylinder. Upper and lower walls of the flow domain are maintained at a distance of 10D from the center of cylinder. A uniform velocity of 0.3149 m/s is applied at the domain inlet, corresponding to the Reynold's Number of 10^4 (where D = 1 m, density = 1000 kg/m3 , and viscosity = 0.03149 kg/m-s). In this research work, all the important physical parameters like Re, m, z and frequency ratio, are non-dimensional in nature. All the dimensionless parameters used in this study are similar to those used by Hover [14] (Experimental study) and Nguyen et al. [13] (Numerical study) which is done by adjusting the values of D, U, ρ, υ, k, m and z.

3.2 Ansys/Fluent

For this numerical study, Ansys Fluent has been selected for the solution of flow around the cylinder. As this software contains the broad physical modeling capabilities needed to model flow, turbulence. From the design of the flow domain to the solution of the fluid flow, all steps have been completed in Ansys Fluent. The summary and setup of the complete process has been explained below:

3.2.1 CAD Model

The CAD model for flow around cylinder is generated using design modular (Ansys Fluent).

Figure 3 shows the details of CAD model generated for this study.

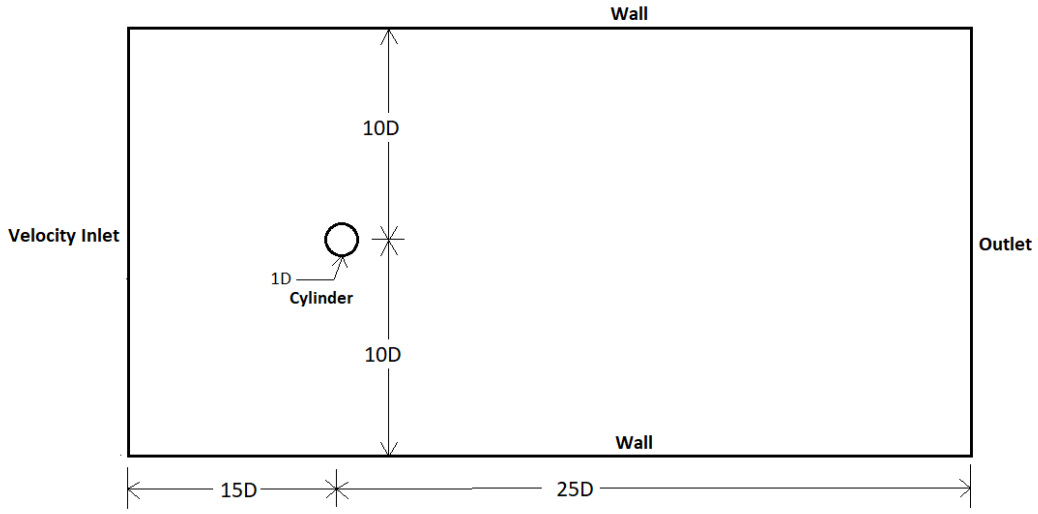

Figure 3. CAD Model with boundary conditions

3.2.2 Mesh:

In all case studies, the computational domain is divided into two zones, to control the stability of the cylinder, the area around the cylinder is meshed using structured quadrilateral elements and the rest is meshed using triangular elements. The mesh is developed in such a way that the region around the wall of the cylinder has a very fine mesh whereas as the region far away from cylinder has a coarse mesh. Figure 4 (a) and (b) represents the mesh and mesh detail section view near cylinder.

The non-dimensionless distance between the first mesh node and cylinder, known as the y+ value, is very important in accurately solving the flow. According to ANSYS [29], the y+ value should be less than or equal to unity to ensure the adequate resolution of the grid near the cylinder in simulation. To ensure the y+ value at unity, the 1st mesh layer height was place at 1.4e-3 from cylinder. Table 3. Shows the mesh details. In the current study, y+ = 1 is maintained in all cases with Ur ranging from 1 to 14.

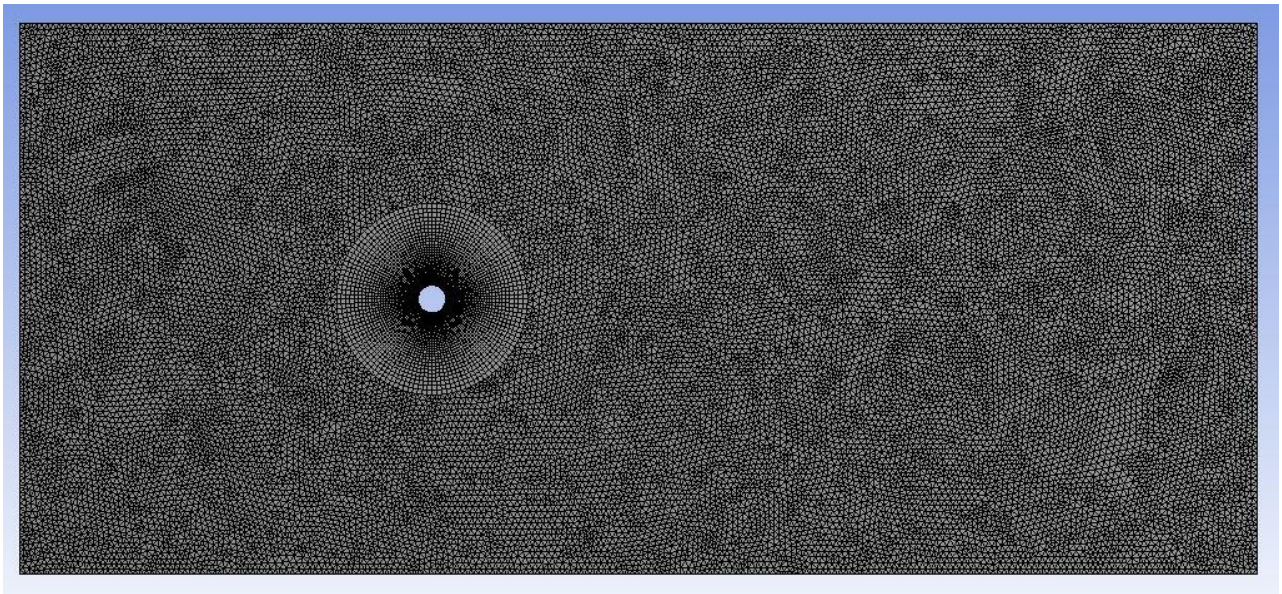

Figure 4. Mesh

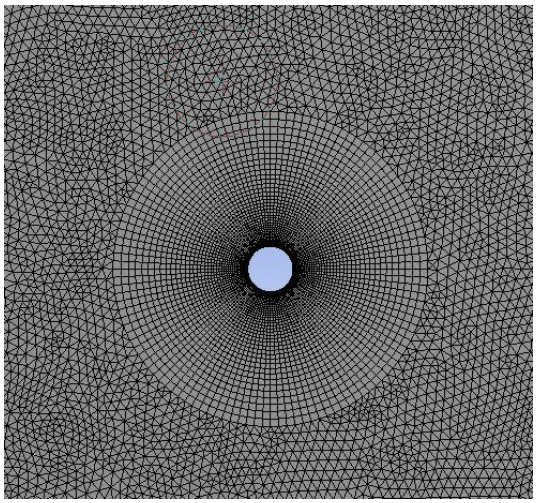

Figure 4. (b) Mesh closeup view near cylinder

Table 3. Mesh details

First layer height	1.4e-3
Total No. of mesh elements	51094

3.3 Grid Independency

The grid independency tests were performed at Re = 10000, m = 11, Ur = 5.84, z = 0.001 and Ks/D = 0 for the results of the maximum cylinder response amplitude (Ay/D) [Table 3]. These grid independency tests were performed at different grid resolutions. Results obtained from these simulations for maximum cylinder response amplitude were validated against the experimental [14] and numerical study [13] performed by Hover and Nguyen respectively. Table 3 presents the results for four different meshes. It was observed that M3 was able to achieve acceptable value of maximum response amplitude and further mesh refinements had negligible impact on the cylinder response. Therefore, M3 was finalized because it provided acceptable results and was even less time consuming than the M4.

Table 4. Grid independency tests with RANS kw-sst Model

Mesh	**No. of elements**	**Maximum Ay/d**	**Experimental Ay/d [14]**	**Numerical Ay/d [13]**
M1	28050	0.52	1.003	0.9230
M2	34980	0.581		
M3	51094	0.6702		
M4	64364	0.6771		

3.4 Boundary Conditions

To meet the requirements for this study, SST k-omega model has been used for pressure based transient flow. It combines the best of the both worlds. The use of a k-ω formulation in the inner parts of the boundary layer makes the model directly usable to the wall through the viscous sub-layer and the SST formulation switches to a k-ε behaviour in the free-stream. Figure 5 shows working of SST k-omega. An average static reference pressure of 0 Pa is applied at the outlet boundary. A symmetric wall condition is applied to the both upper and lower walls of flow domain. To investigate the boundary layer separation and vortex generation phenomenon, a No-slip condition is assigned to cylinder wall. The result of applying No-slip condition is that the velocity near the cylinder wall would be zero and moving away from the cylinder it will increase to the freestream velocity.

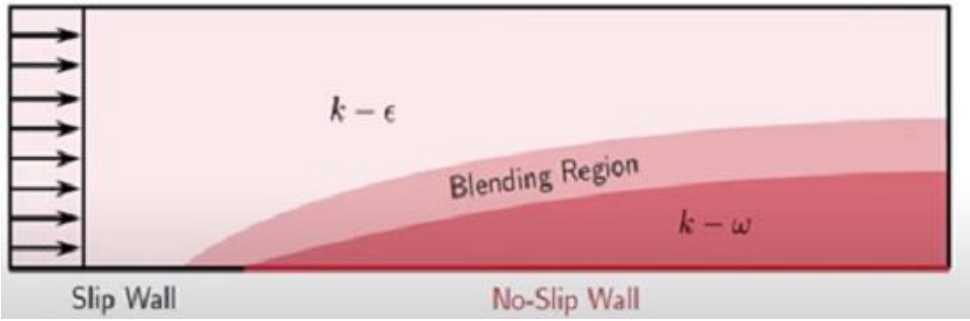

Figure 5. SST k-omega

Dynamic Mesh

In Ansys fluent, an option called dynamic mesh is used for simulation of problems with boundary motion. By the use of a User Defined Function (UDF) the motion of the circular cylinder can be calculated from the integrated forces and stress exported from Fluent Solver. The UDF calculates the new position of the cylinder and exports back to the solver and a new iteration start. Diffusion-based smoothing method is used here for dynamic. Diffusion produces better quality mesh and allows cylinder oscillations of high amplitude without any limitation on the direction of motion.

Pressure-Velocity coupling

ANSYS Fluent provides four types of Pressure-Velocity coupling algorithms: SIMPLE, SIMPLEC, PISO, COUPLED and for time-dependent flows using the Non-Iterative Time Advancement option (NITA) Fractional Step (FSM). A considerably high amount of computational power is required for all these algorithms, therefore, Non-Iterative Time Advancement option (NITA) Fractional Step (FSM) scheme is used mostly for the unsteady flow simulation.

The details of all the input boundary conditions are shown in Table 5.

Table 5: Input boundary conditions

Solver type /time	Pressure based /transient
Models	SST k-omega
Materials	Density = 1000 kg/m3 Viscosity = 0.03149 kg/m-s
Cell zone condition	Operating pressure=0
Boundary conditions (Inlet)	Velocity Inlet Velocity=0.031
Boundary conditions (Outlet)	Pressure outlet Pressure=transient tabular data
Dynamic Mesh	Mesh method= Smoothing/Diffusion Diffusion parameter=1.5 6-DOF
Solution method	Coupling = Fractional step Formulation = First order NITA
Solution control	Courant number is mmaintained below 1
Monitors	Coefficient of lift and coefficient of drag
Solution initialize	Standard
Run calculation	Step size=0.004 (Smooth Cylinder) Step size=0.1 (Rough Cylinder)

Chapter 4 Oscillating cylinder

4.1 Smooth cylinder

4.1.1 Mass ratio 11

The smooth cylinder is allowed to oscillate in the transverse direction only where its displacement is induced by vortex shedding from the cylinder. The cylinder is constrained by a spring–damper system with spring constant k and damping coefficient c as shown in Fig 2. A uniform velocity of 0.3149 m/s is applied at the domain inlet, corresponding to the Reynold's Number of 10^4 (where D = 1 m, density = 1000 kg/m3, and viscosity = 0.03149 kg/m-s). All the parameters used in this case study are just the same as used by Hover [14] and Nguyen [13]. All the simulations are performed at a subcritical Reynold's Number (Re) = 10^4, mass ratio = 11, damping z = 0.001 and are carried out in the reduced velocities range of $2 \leq Ur \leq 14$. The change in the reduced velocity is achieved by changing the natural frequency f_n of the cylinder.

Results & discussion

At mass ratio=11, 6 simulations were performed for reduced velocities of Ur=2.5, 3.78, 5.84, 7.52, 8.77 & 11, corresponding amplitude responses, vortex shapes and force coefficients were recorded. The fluctuating lift force acting on the cylinder from vortex shedding induces periodic displacement, possibly resulting in generation of various wake patterns as reported by Williamson and Govardhan [32]. The time histories of non-dimensional amplitude response and force coefficients are shown in Fig 8 and Fig 13 respectively. At reduced velocity of Ur=2.5 which lies in the initial branch, it was observed that amplitude response of the cylinder is very small. In addition to that, very small values of drag force were observed.

As the reduced velocity is increased to Ur=3.78, a significant increase in amplitude response (Ay/D = 0.22) was measured which is high in comparison to the results reported by Hover [14] and Nguyen [13] as shown in Fig 6. A 2S vortex mode was observed in the wake region at Ur=3.78, comprising of two single vortices per cycle into the wake region as shown in Fig. 9. Which agrees well with the literature and it has been validated by Niaz [15]. The maximum value of amplitude response was observed to be Ay/D = 0.67 at Ur = 5.84 which lies in the upper branch. In the wake region, 2P mode of vortex shedding comprising of two vortex pairs per cycle into the wake region was observed. It can be seen in Fig. 10. Which corresponds to high amplitude response and is observed in upper branch at peak amplitude response as reported by Williamson and Govardhan [32]. This 2P vortex mode has

already been recorded by Nguyen [13] and Niaz [15]. In the upper branch, higher values of drag were observed which can be seen in Fig 13. This agrees well with literature and has been reported by Bishop and Hassan [42].

At Ur=7.52, the amplitude response was observed to be very small (Ay/D = 0.15) in comparison to the results reported by Hover [14]. With an increase in reduced velocity to Ur=8.77, the amplitude response decreased to a small value of Ay/D = 0.1 which is also a little lower in comparison to the results reported by Hover [14] and Nguyen [13]. Vortex mode of 2S was observed in the wake region at both Ur=7.52 and Ur=8.77 which agrees well with the literature as recorded by by Niaz [15]. Vortex modes for both Ur=7.52 and Ur=8.77 can be seen in Fig 11 and fig 12 respectively. At Ur=11, the amplitude response was observed to be very small (Ay/D = 0.04) which agrees well with the results reported by Hover [14]. It was observed that at initial branch and lower branch where amplitude response is very small, drag forces also appear to be very small values. Which agrees well with the literature. It has been reported by Bishop and Hassan [42] that during lock-in region drag forces are high and out of lock-in region drag forces are low.

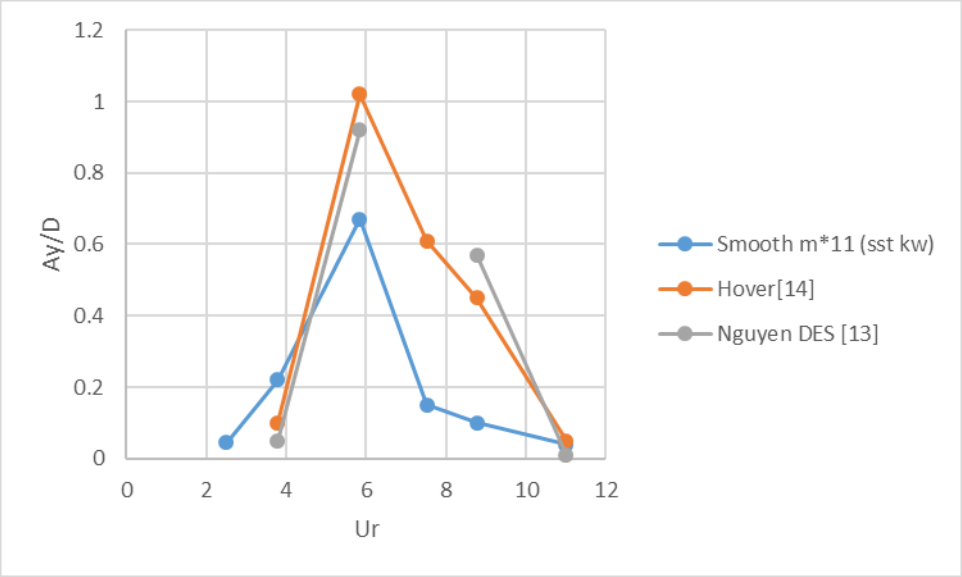

Figure 6. Comparison of amplitude response (m* = 11, ζ = 0.001, Re = 10000)

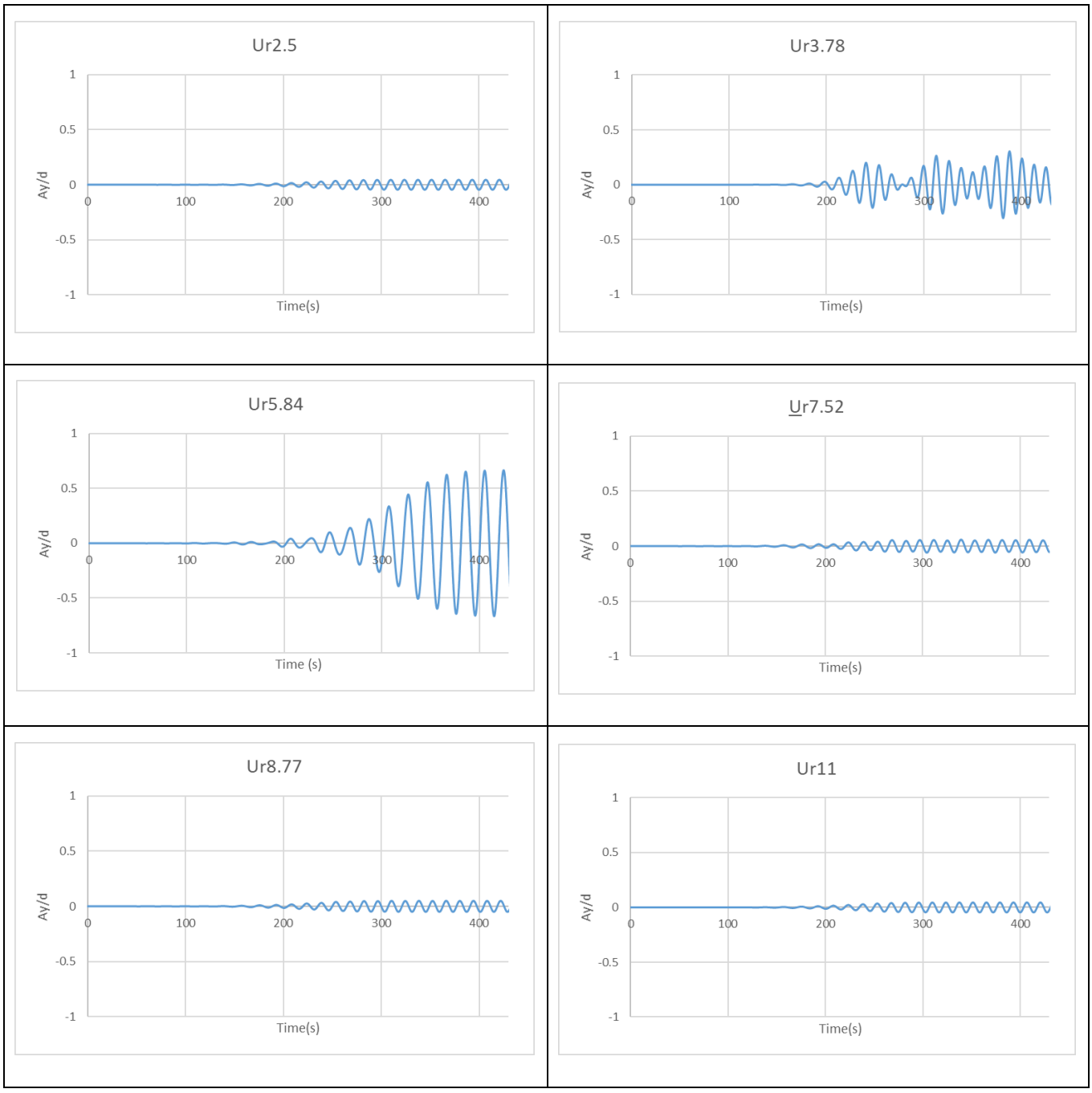

Figure 8. Time history of amplitude responses at reduced velocities (Ur=2.5, 3.78, 5.84, 7.52, 8.77 & 11)

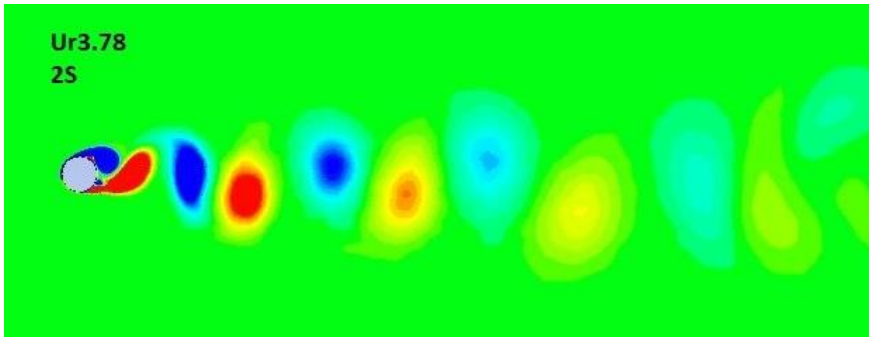

Figure 9. Vorticity contour at Ur= 3.78

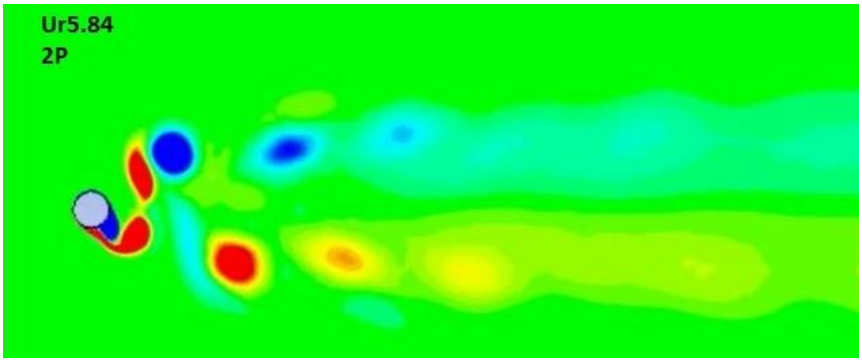

Figure 10. Vorticity contour at Ur=5.84

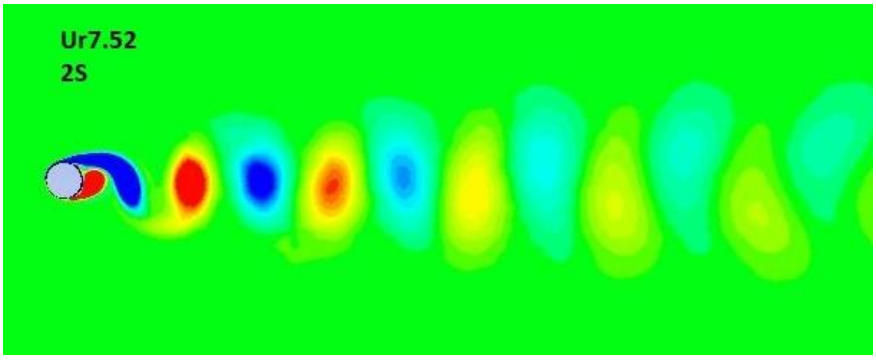

Figure 11. Vorticity contour at Ur=7.52

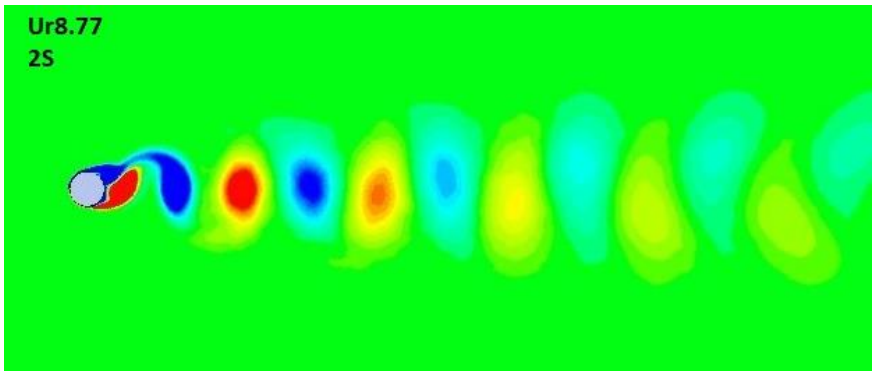

Figure 12. Vorticity contour at Ur=8.77

Figure 13. Time history of force coefficients (cd & cl) at (Ur=2.5, 3.78, 5.84, 7.52, 8.77 & 11)

Conclusion

The study was performed for investigation of the VIV phenomenon, for an elastically mounted rigid cylinder free to oscillate in traverse direction direction at mass ratio (m* = 11), z = 0.001 and Ur = 2 to 14 with Reynolds number fixed at Re = 10^4. The study was conducted to test the capability of 2d RANS approach and kw-SST model. The results were validated against the results of a 3-dimensional numerical study using DES model and an experimental study. It was found from the study that kw-SST was successful in capturing all three branch responses (Initial branch, Upper branch and lower branch) and it also successfully captured 2S & 2P vortex modes for the corresponding amplitude responses and their branches. However, peak amplitude responses were a little lower in comparison to the numerical (DES model) and experimental study which could be explained due to lower aspect ratio of mesh. But comparatively, the study was computationally less expensive and was also less time consuming, which concludes that 2D RANS approach and kw-SST turbulent model is quite reliable and capable for the resolution of complex fluid flow problems.

4.1.2 Mass ratio 2.4

All the parameters used in this case study are just the same as used in previous study except mass ratio, which in this case is m*=2.4. A uniform velocity of 0.3149 m/s is applied at the domain inlet, corresponding to the Reynold's Number of 10^4 (where D = 1 m, density = 1000 kg/m3, and viscosity = 0.03149 kg/m-s). All the simulations are performed at a subcritical Reynold's Number (Re) = 10^4, mass ratio = 2.4, damping z = 0.001 and are carried out in the reduced velocities range of $2 \leq Ur \leq 14$.

Results & discussion

The study for mass ratio=2.4 has been performed at reduced velocities in the range of $2 \leq Ur \leq 14$. The time histories of non-dimensional amplitude response and force coefficients are shown in Fig 14 and Fig 19 respectively. In the initial branch at reduced velocity of Ur=2.5, the amplitude response of the cylinder was observed to be (Ay/D = 0.23) which is relatively very small. In addition to that, drag forces acting on cylinder were also observed to be small.

With an increase in reduced velocity to Ur=3.78, a significant increase in amplitude response (Ay/D = 0.62) was measured which is relatively very high in comparison to the response observed for m*=11 in the previous case. Pan et al. [11] reported amplitude response of Ay/d=0.30 and a 2s vortex shedding mode at m*=2.4 (Ur=3.93, Re=3400). But a higher amplitude response and P+S vortex mode was

observed in the wake region at Ur=3.78, Re=10000 comprising of one pair and one single vortex shedding into the wake occur during each half cycle, as shown in Fig 15. A very high drag response was observed which agrees well with the literature as reported by reported by Bishop and Hassan [42]. At Ur = 5.84, the maximum value of amplitude response was observed to be Ay/D = 0.73, which lies in the upper branch, the amplitude response was very high in comparison to the case study at m*=11. This behavior shows good agreement with the literature and has been already reported by B. Stappenbelt [22] and Alireza modir [23]. The maximum amplitude response for Ur=5.84 can be seen in Fig 14. In the wake region, 2P mode of vortex shedding comprising of two vortex pairs per cycle into the wake region was observed. It can be seen in Fig 16. Which corresponds to high amplitude response and is observed in upper branch at peak amplitude response as reported by Williamson and Govardhan [32]. In the upper branch, higher values of drag were observed which can be seen in Fig 18. This agrees well with literature and has been reported by Bishop and Hassan [42].

At Ur=7.52, the amplitude response was observed to be (Ay/D = 0.53) which is very high in comparison to the amplitude response at m*=11. Vortex mode of 2P was observed in the wake region at Ur=7.52 as shown in Fig, which is due to high amplitude response as suggested by Williamson and Govardhan [32]. With an increase in reduced velocity to Ur=8.77, the amplitude response decreased to a small value of Ay/D = 0.165. Vortex mode of 2T was observed in the wake region at Ur=8.77 which agrees well with the literature. Williamson and Govardhan [32] found that 2T vortex mode is also known to cause free vibration, at moderate Re, for mass ratios, m* < 6. This vortex mode, consists of triplet vortices that form in each half cycle as shown in Fig 18. High drag forces were observed at both Ur=7.52 and Ur=8.77 as shown in Fig 19. At Ur=11, the amplitude response was observed to be very small (Ay/D = 0.058). It was observed that at reduced velocities where amplitude response is very small, drag forces also appear to be very small values. Which agrees well with the literature. It has been reported by Bishop and Hassan [42] that during lock-in region drag forces are high and out of lock-in region drag forces are low. In comparison with mass ratio (m*=11), it was found that with decrease in mass ratio the lock-in region widened and there was a significant increase in the cylinder amplitude response as shown in Fig 20. This behavior has been reported by B. Stappenbelt [22] and Alireza modir [23]. The results show good agreement with literature.

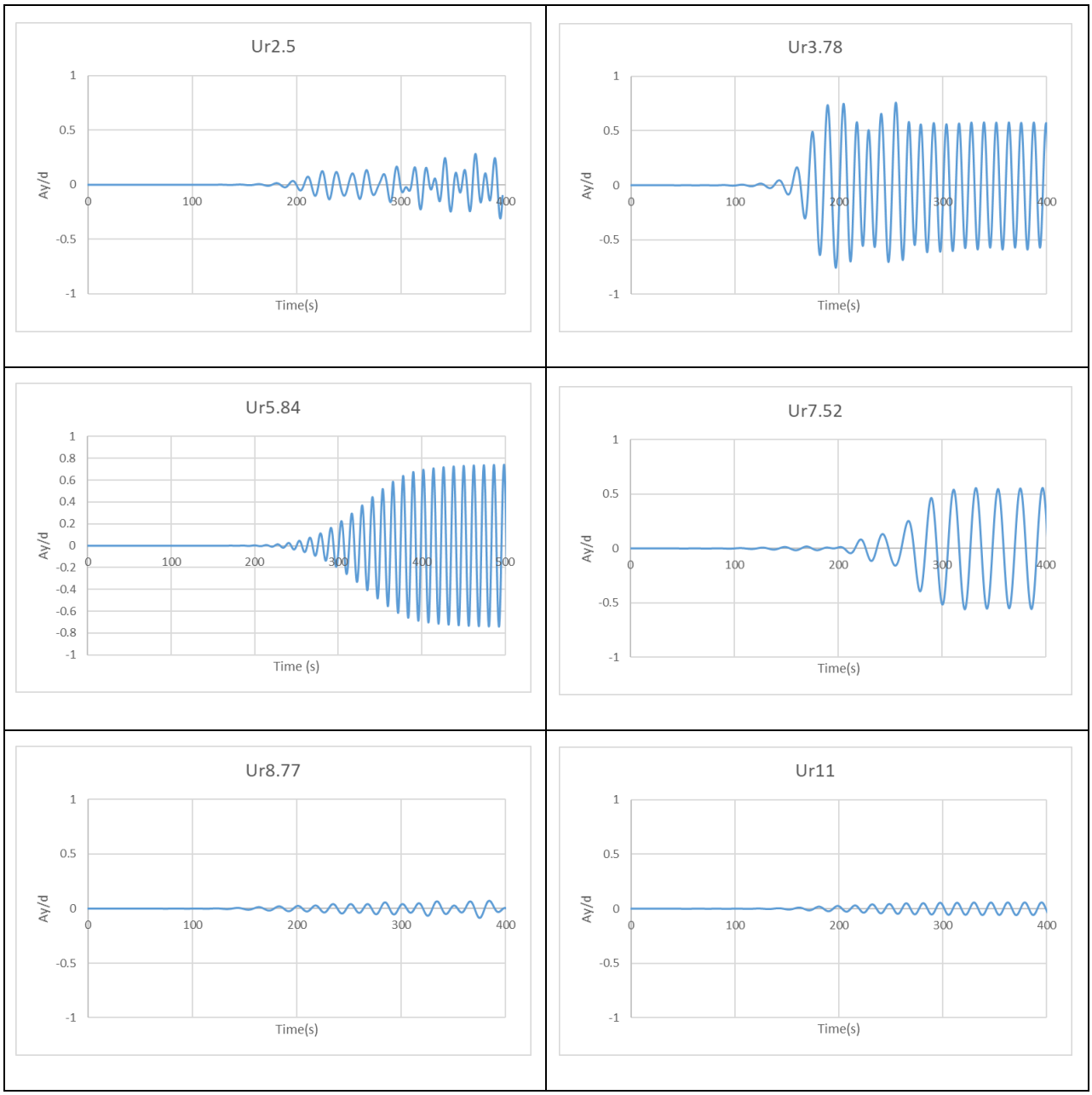

Figure 14. Time history of amplitude responses at reduced velocities (Ur=2.5, 3.78, 5.84, 7.52, 8.77 & 11)

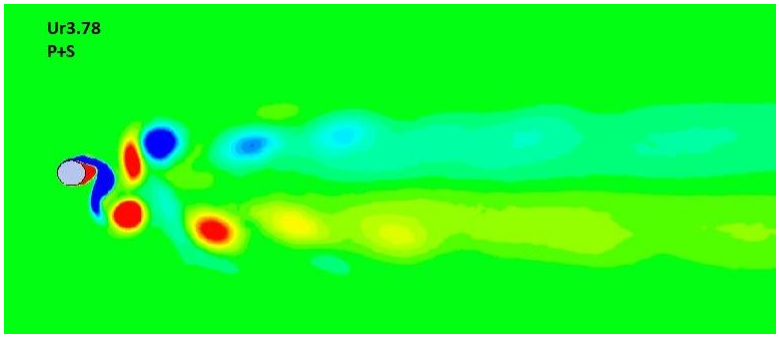

Figure 15. Vorticity contour at Ur= 3.78

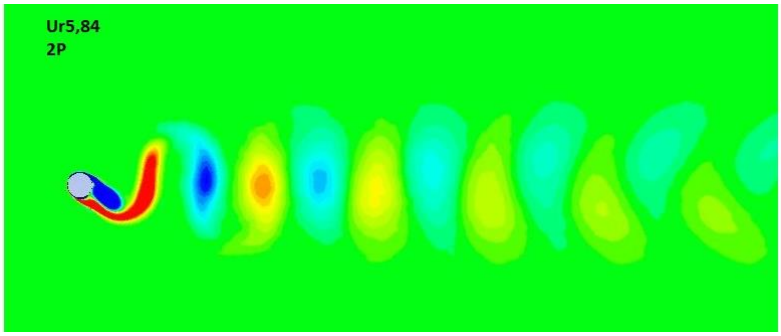

Figure 16. Vorticity contour at Ur= 5.84

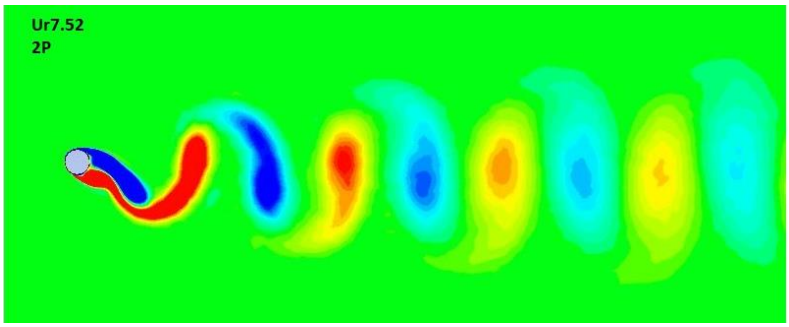

Figure 17. Vorticity contour at Ur= 7.52

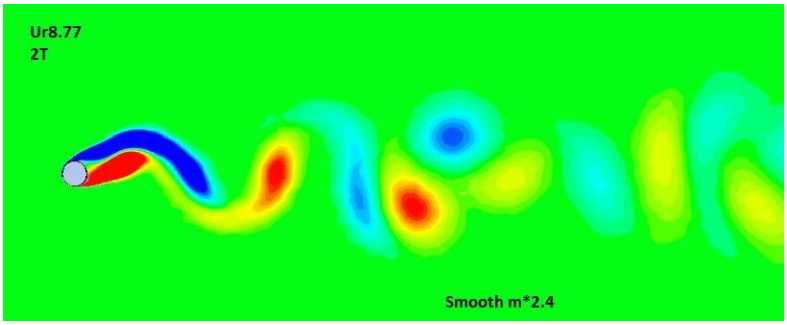

Figure 18. Vorticity contour at Ur= 8.77

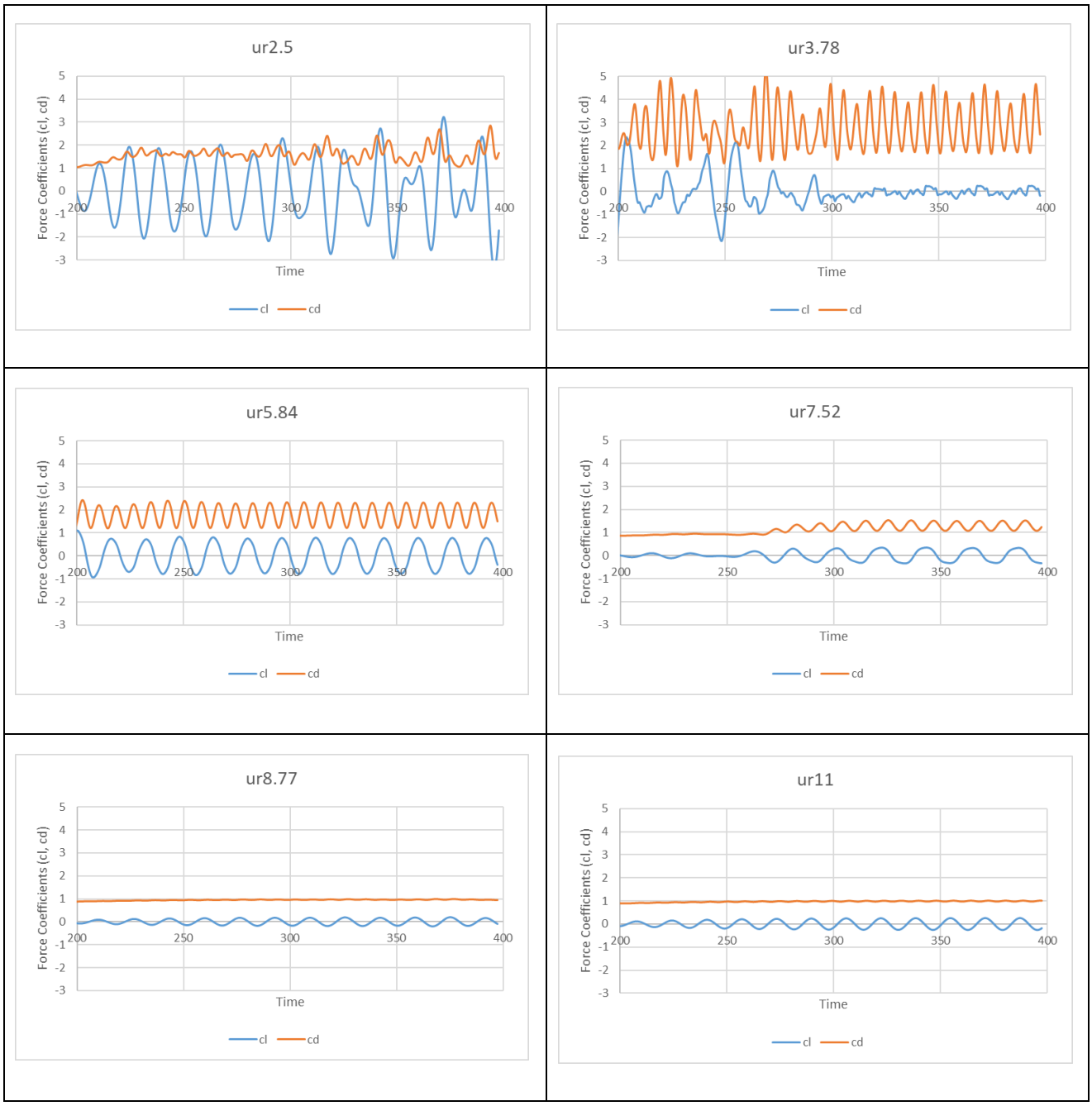

Figure 19. Time history of force coefficients (cd & cl) at (Ur=2.5, 3.78, 5.84, 7.52, 8.77 & 11)

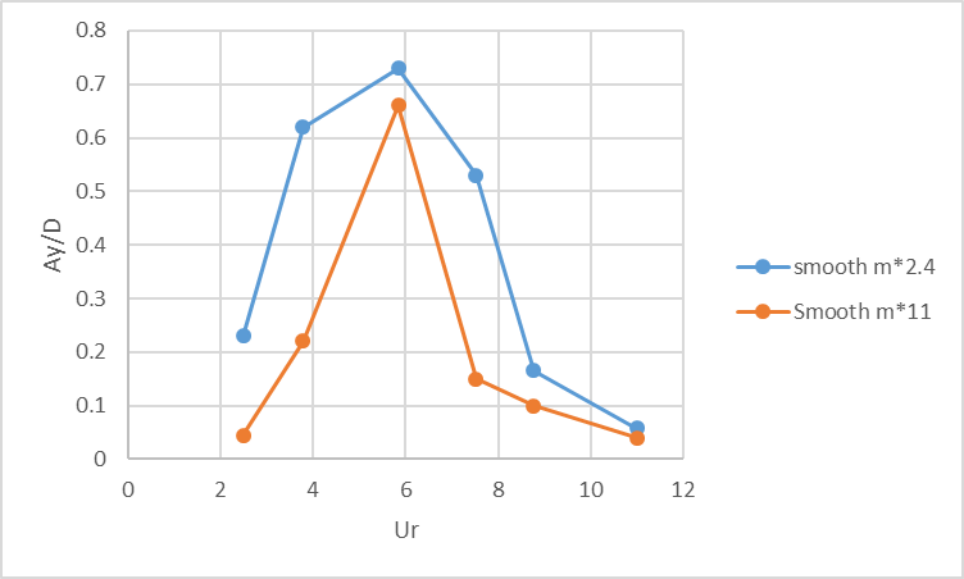

Figure 20. Comparison of amplitude response for smooth cylinders at (m* = 11 & m* = 2.4)

Conclusion

The study was performed to investigate the impact of mass ratio on vortex shape, crossflow amplitude and lock-in region. The study was performed at mass ratio, m*=2.4 with the same 1-DOF vibrating system and parameters. The results obtained from this study were compared with results obtained at m*=11 and literature review. It was found that with decrease in mass ratio the lock-in region widened and there was a significant increase in the cylinder amplitude response. This behavior has been reported in literature in previous numerical and experimental studies. With decrease in mass ratio, vortex modes of P+S, 2P & 2T appeared at reduced velocities ranging from Ur = 2 to 14. These vortex modes correspond to high amplitude responses and their appearance in wake region at low mass ratios and high Reynolds number has been reported in literature. The results show good agreement with literature.

4.2 Rough Cylinder

The VIV phenomenon for rough cylinder is studied at 2 different mass ratios (m*=2.4 & 11). For this study the roughness height (Ks) 0.02D is used. Fig 21 shows the schematic diagram of equivalent sand model. For Ansys to incorporate this roughness height, the size of roughness element should be less than the centroid of first mesh node as shown in Fig 22. To incorporate this roughness height first layer height for mesh is changed from 1.4e-3 to 0.006. The adjusted mesh for rough cylinder can be seen in Fig 23.

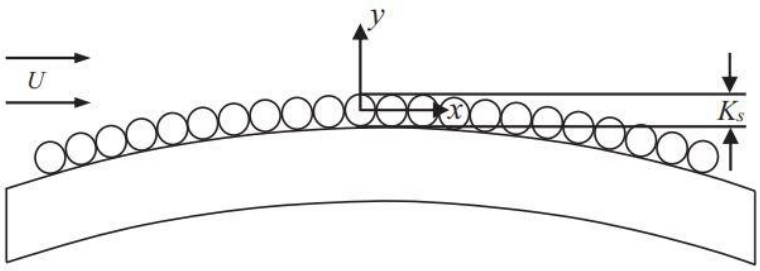

Figure 21. Schematic diagram of equivalent sand model

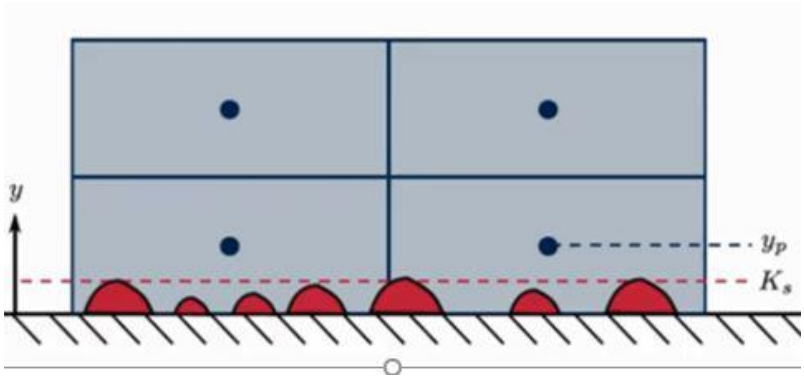

Figure 22. Schematic diagram for Roughness height

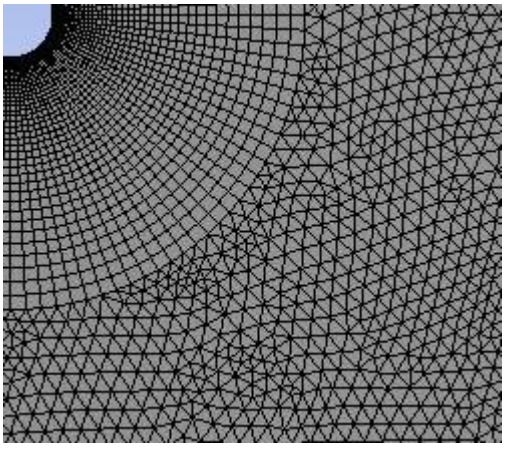

Figure 23. Adjusted mesh

4.2.1 Mass ratio 2.4

This case study was performed for a rough cylinder with a roughness height (Ks) of 0.02D rare at mass ratio, m*=2.4. A uniform velocity of 0.3149 m/s is applied at the domain inlet, corresponding to the Reynold's Number of 10^4 (where D = 1 m, density = 1000 kg/m3, and viscosity = 0.03149 kg/m-s). All the simulations are performed at a subcritical Reynold's Number (Re) = 10^4, mass ratio = 2.4, damping z = 0.001 and are carried out in the reduced velocities range of $2 \leq Ur \leq 14$.

Results & discussion

The study for the rough cylinder at mass ratio, m*=2.4 has been performed at reduced velocities in the range of $2 \leq Ur \leq 14$. The results are compared with that of smooth cylinder at mass ratio, m*=2.4. Fig 21 shows the comparison of amplitude responses for a smooth cylinder and a rough cylinder at m*=2.4. The time histories of non-dimensional amplitude response and force coefficients are shown in Fig 22 and Fig 27 respectively. At reduced velocity of Ur=2.5, the amplitude response of the cylinder was observed to be (Ay/D = 0.08) which is relatively small in comparison to that of smooth cylinder. Drag forces and lift forces acting on cylinder were also observed to be small.

As the reduced velocity is increased to Ur=3.78, a significant increase in amplitude response (Ay/D = 0.64) was measured which is almost the same as observed for smooth cylinder at m*=2.4 in the previous case. A similar 2P vortex mode was observed in the wake region as observed for the smooth cylinder, comprising of one pair and one single vortex shedding into the wake occur during each half cycle, as shown in Fig 23. A lower cd and a higher cl response were observed in comparison to smooth cylinder. At Ur = 5.84, the value of amplitude response was observed to be Ay/D = 0.51, which is relatively lower in comparison to that of smooth cylinder. 2T vortex mode was observed in the wake region as shown in Fig 24. Whereas 2P vortex mode was observed for smooth cylinder. Which agrees well with the literature, formation of 2T vortex mode in the wake region of rough cylinders was also reported by X. Han [36] at m*=2.6 and moderate RE regimes. In the lock-in region, higher values of drag were observed which can be seen in Fig 27. This agrees well with literature and has been reported by Bishop and Hassan [42].

At Ur=7.52, the amplitude response was observed to be (Ay/D = 0.021) which is very small in comparison to the amplitude response at m*=2.4 for smooth. The formation of 2T was inhibited at higher reduced velocities due to surface roughness. 2S vortex mode was observed in the wake region at Ur=7.52 as shown in Fig 25. With an increase in reduced velocity to Ur=8.77, the amplitude response

decreased to a small value of Ay/D = 0.015. Vortex mode of 2S was observed in the wake region at Ur=8.77 as shown in Fig 26. At Ur=11, the amplitude response was observed to be very small (Ay/D = 0.013). During lock-in region drag forces were found to be high and out of lock-in region drag forces were low. Which agrees well with literature and it has been reported by Bishop and Hassan [42]. It was found that surface roughness narrowed the lock-in region and decreased the cylinder amplitude response. Which agrees well with the literature and has been reported by Y. Gao [21], Mohd Ghazali [34] & X. Han [36]. It was found from the study that besides narrowing of the lock-in region, the lock-in region was shifted towards lower reduced velocities, a similar trend has also been observed in the numerical studies of Y. Gao [21] & X. Han [36].

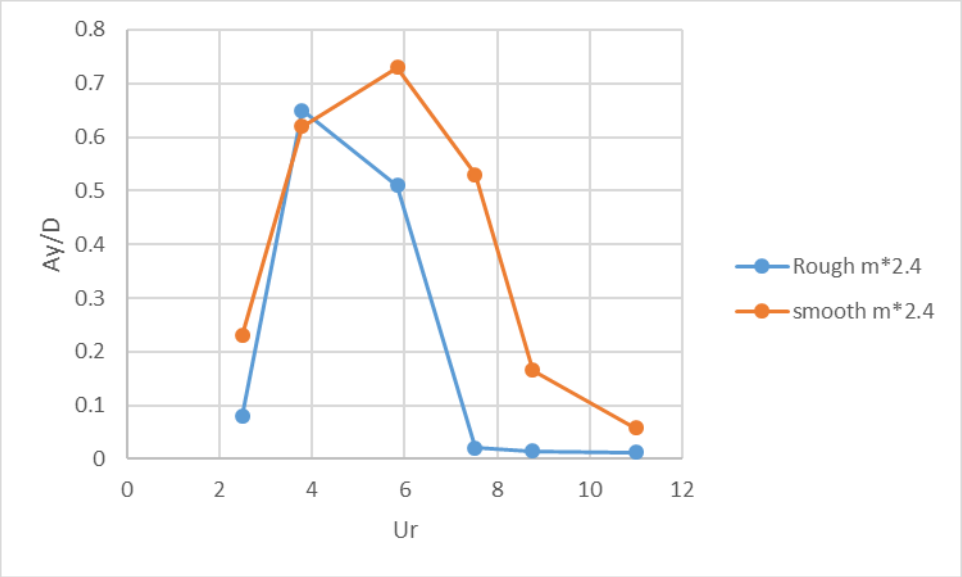

Figure 21. Comparison of amplitude responses for a smooth cylinder and a rough cylinder (i.e., Ks/ D=2×10−2) at m* = 2.4

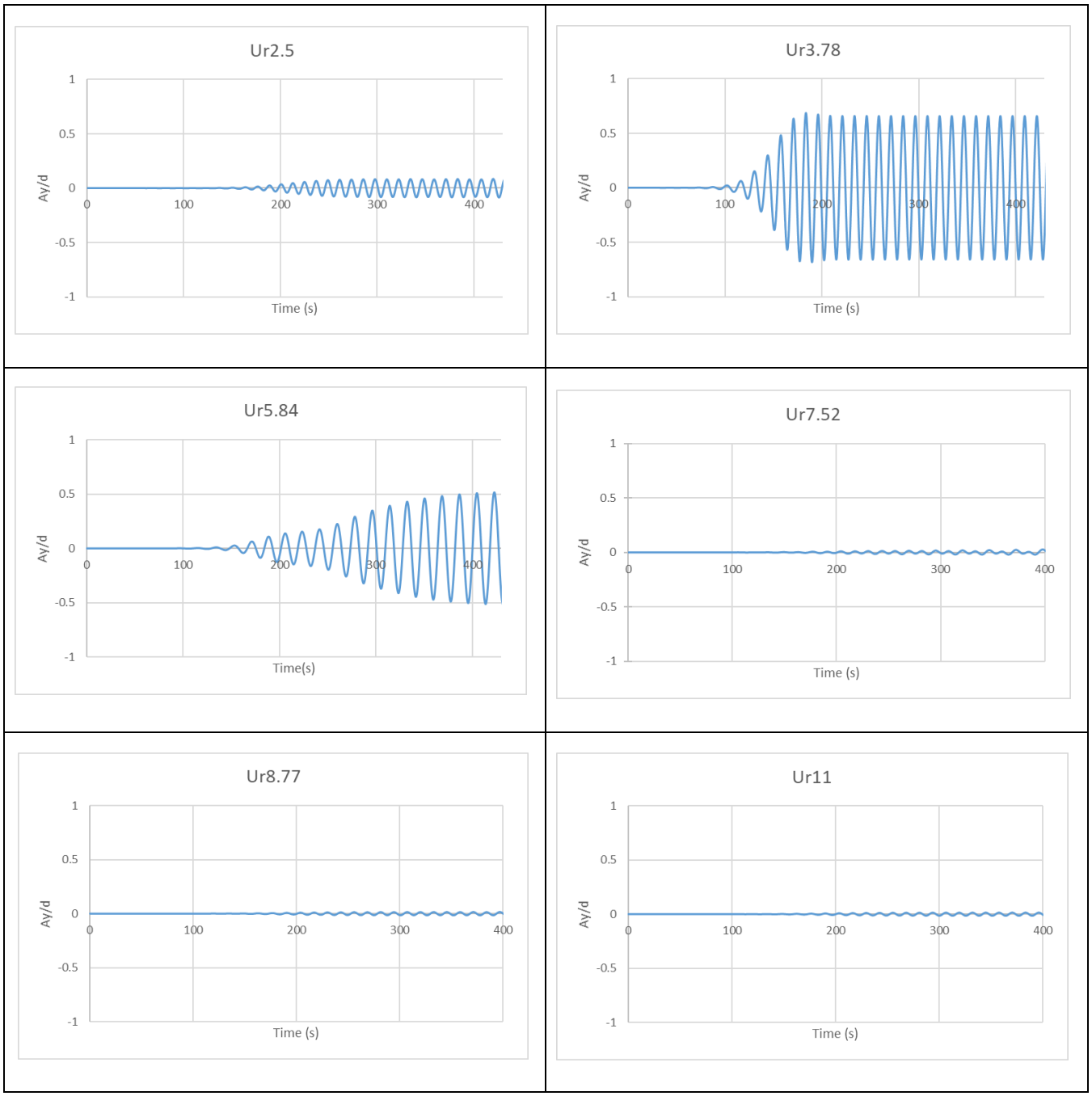

Figure 22. Time history of amplitude responses at reduced velocities (Ur=2.5, 3.78, 5.84, 7.52, 8.77 & 11)

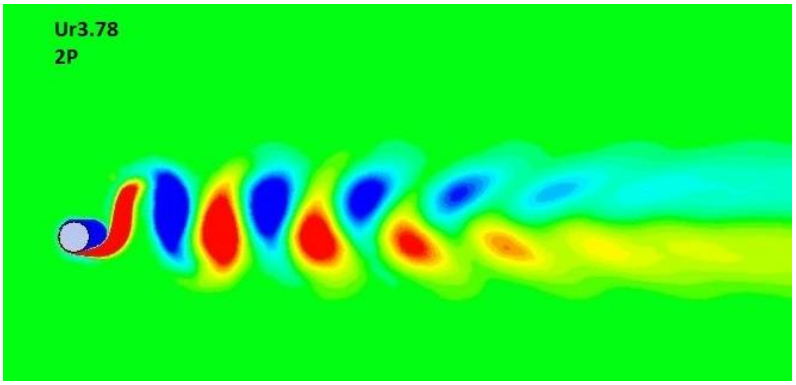

Figure 23. Vorticity contour at Ur= 3.78

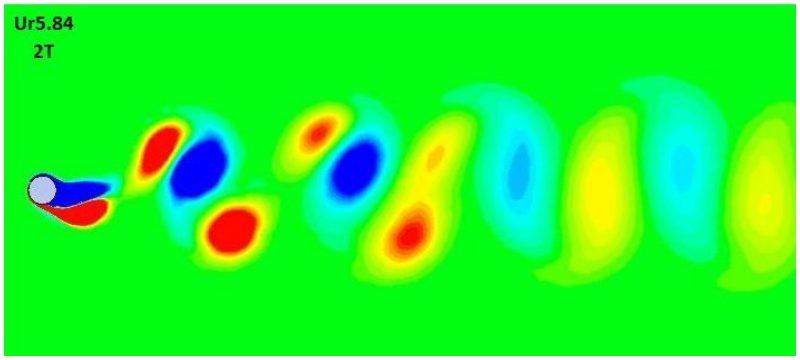

Figure 24. Vorticity contour at Ur= 5.84

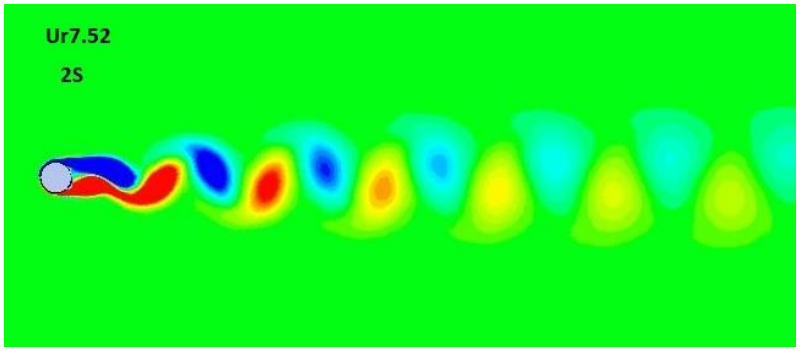

Figure 25. Vorticity contour at Ur= 7.52

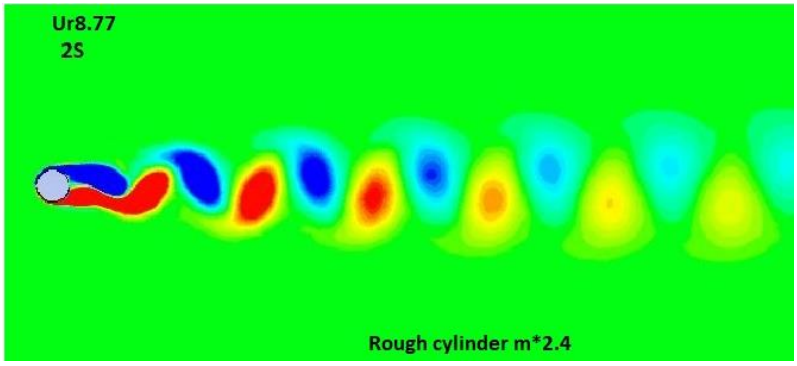

Figure 26. Vorticity contour at Ur= 8.77

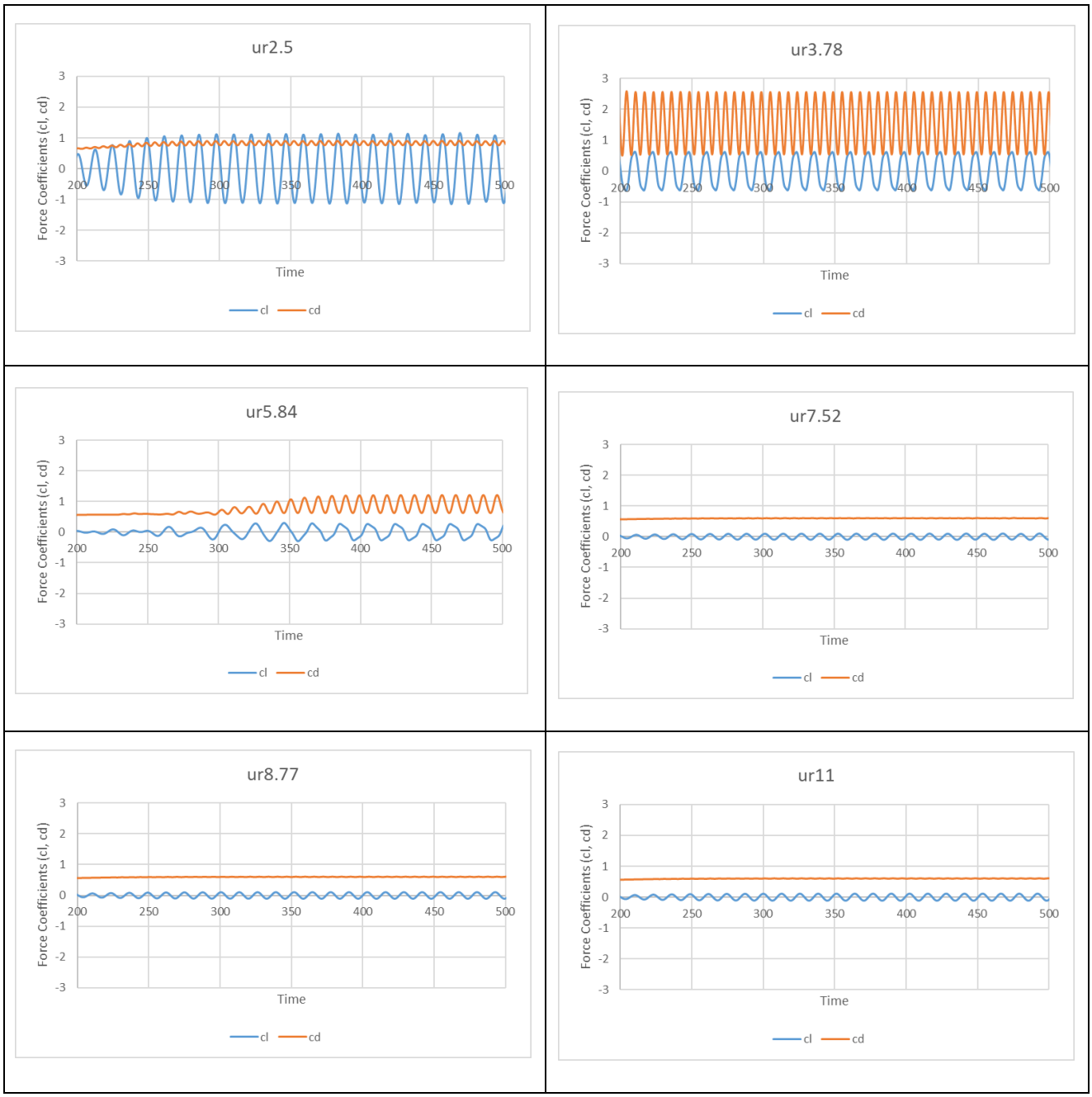

Figure 27. Time history of force coefficients (cd & cl) at (Ur=2.5, 3.78, 5.84, 7.52, 8.77 & 11)

Conclusion

The study was performed to investigate the impact of surface roughness on vortex shape, crossflow amplitude and lock-in region. The study was performed for a rough cylinder (i.e., Ks/ D=2×10−2) at mass ratio, m*=2.4. The results obtained from this study were compared with that of smooth cylinder.

All the parameters in both cases for kept same. It was found that rough cylinder had a narrower lock-in region and reduced amplitude response. As a result of surface roughness, the lock-in region was shifted towards low reduced velocities. 2P & 2T vortex modes at low reduced velocities at high amplitude responses. Formation of these vortex modes have also been reported in literature for rough cylinder. At higher reduced velocities, low amplitude response was observed with the formation of 2S vortex mode in the wake. It was observed lift forces decreased with increase in reduced velocity, drag forces were found to be high in lock-in region & low in out of lock-in region.

4.2.2 Mass ratio 11

This case study was performed for a rough cylinder with a roughness height (Ks) of 0.02D rare at mass ratio, m*=11. A uniform velocity of 0.3149 m/s is applied at the domain inlet, corresponding to the Reynold's Number of 10^4 (where D = 1 m, density = 1000 kg/m3, and viscosity = 0.03149 kg/m-s). All the simulations are performed at a subcritical Reynold's Number (Re) = 10^4, mass ratio = 11, damping z = 0.001 and are carried out in the reduced velocities range of $2 \leq Ur \leq 14$.

Results & discussion

The study for the rough cylinder at mass ratio, m*=11 has been performed at reduced velocities in the range of $2 \leq Ur \leq 14$. The results are compared with that of smooth cylinder at mass ratio, m*=11. Fig 28 shows the comparison of amplitude responses for a smooth cylinder and a rough cylinder at m*=11. The time histories of non-dimensional amplitude response and force coefficients are shown in Fig 29 and Fig 34 respectively. At reduced velocity of Ur=2.5, the amplitude response of the cylinder was observed to be (Ay/D = 0.0065) extremely small in comparison to that of smooth cylinder at m*=11. Drag forces and lift forces acting on cylinder were also observed to be small.

As the reduced velocity is increased to Ur=3.78, a significant increase in amplitude response (Ay/D = 0.53) was measured which is high in comparison to smooth cylinder at m*=11 in the previous case. 2P vortex mode was observed in the wake region as shown in Fig 30. Whereas 2S mode of vortex shedding was observed for the smooth cylinder at m*=11.The values of cd and cl were found to be very high at this peak amplitude response. In the lock-in region, higher values of drag were observed which can be seen in Fig 34. This agrees well with literature and has been reported by Bishop and Hassan [42].

At Ur = 5.84, the value of amplitude response was observed to be Ay/D = 0.015, which is extremely small in comparison to that of smooth cylinder. 2S vortex mode was observed in the wake region as

shown in Fig 31. Whereas 2P vortex mode was observed for smooth cylinder (m*=11) at Ur= 5.84, formation of 2P vortex mode was inhibited due to surface roughness. Which agrees well with the literature, such inhibition phenomenon has also been reported by X. Han [36] at m*=2.6 and moderate RE regimes.

At Ur=7.52, the amplitude response was observed to be (Ay/D = 0.0092) which is very small in comparison to the amplitude response at m*=11 for smooth cylinder. 2S vortex mode was observed in the wake region at Ur=7.52 as shown in Fig 32. With an increase in reduced velocity to Ur=8.77, the amplitude response decreased to a small value of Ay/D = 0.0074. Vortex mode of 2S was observed in the wake region at Ur=8.77 as shown in Fig 33. At Ur=11, the amplitude response was observed to be very small (Ay/D = 0.0064). It was found that surface roughness narrowed the lock-in region and decreased the cylinder amplitude response. Which agrees well with the literature and has been reported by Y. Gao [21], Mohd Ghazali [34] & X. Han [36]. It was found from the study that besides narrowing of the lock-in region, the lock-in region was shifted towards lower reduced velocities, a similar trend has also been observed in the numerical studies of Y. Gao [21] & X. Han [36].

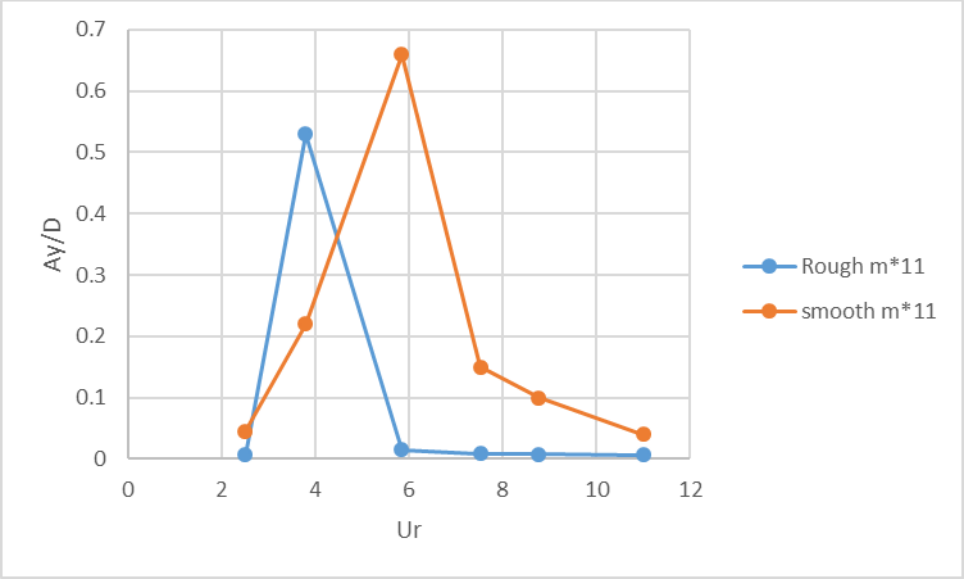

Figure 28. Comparison of amplitude responses for a smooth cylinder and a rough cylinder (i.e., Ks/ D=2×10−2) at m* = 11

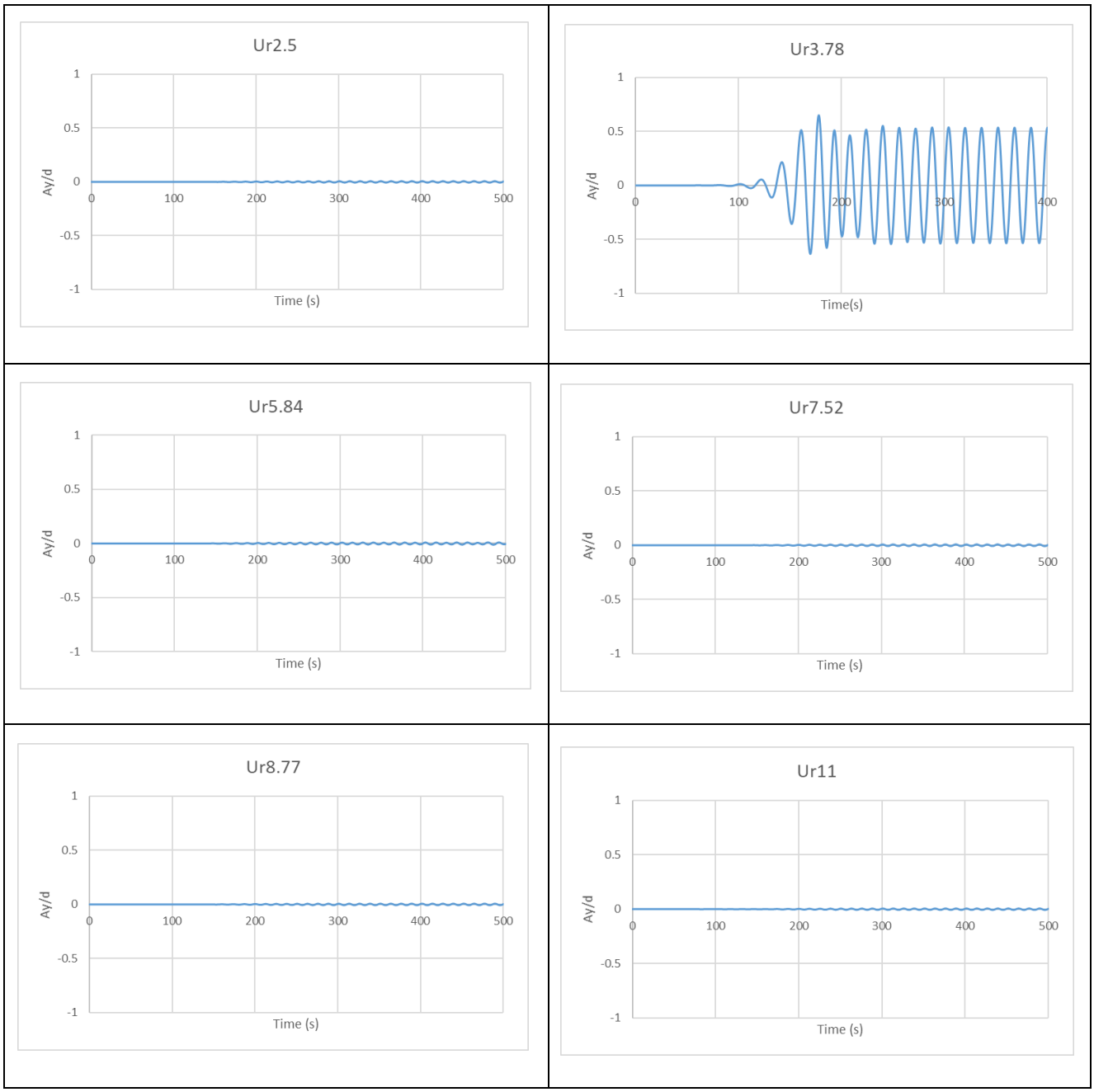

Figure 29. Time history of amplitude responses at reduced velocities (Ur=2.5, 3.78, 5.84, 7.52, 8.77 & 11)

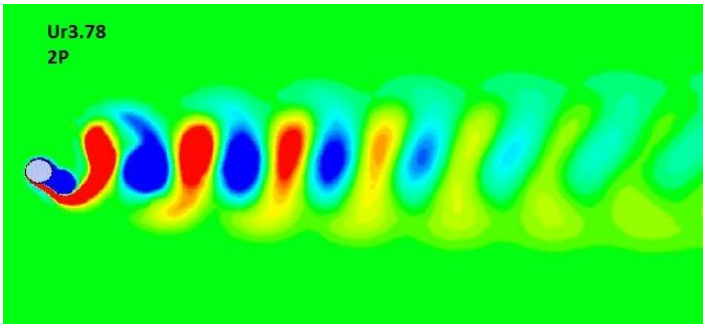

Figure 30. Vorticity contour at Ur= 3.78

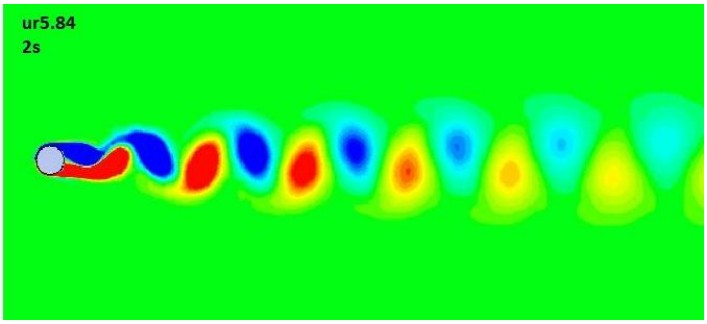

Figure 31. Vorticity contour at Ur= 5.84

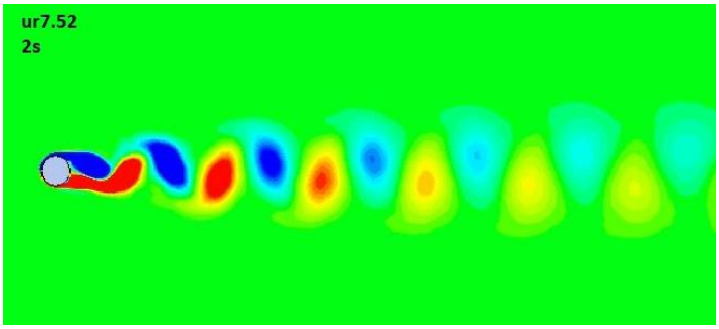

Figure 32. Vorticity contour at Ur= 7.52

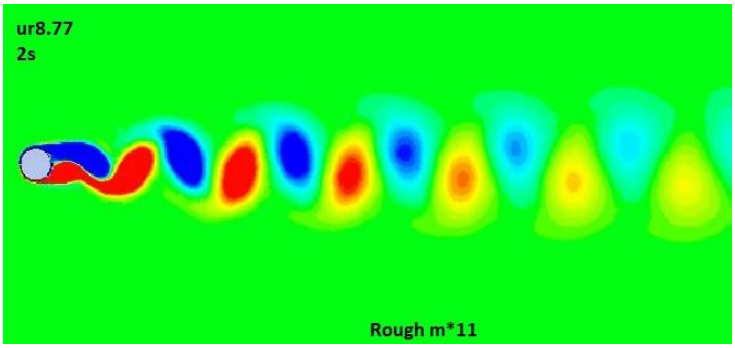

Figure 33. Vorticity contour at Ur= 8.77

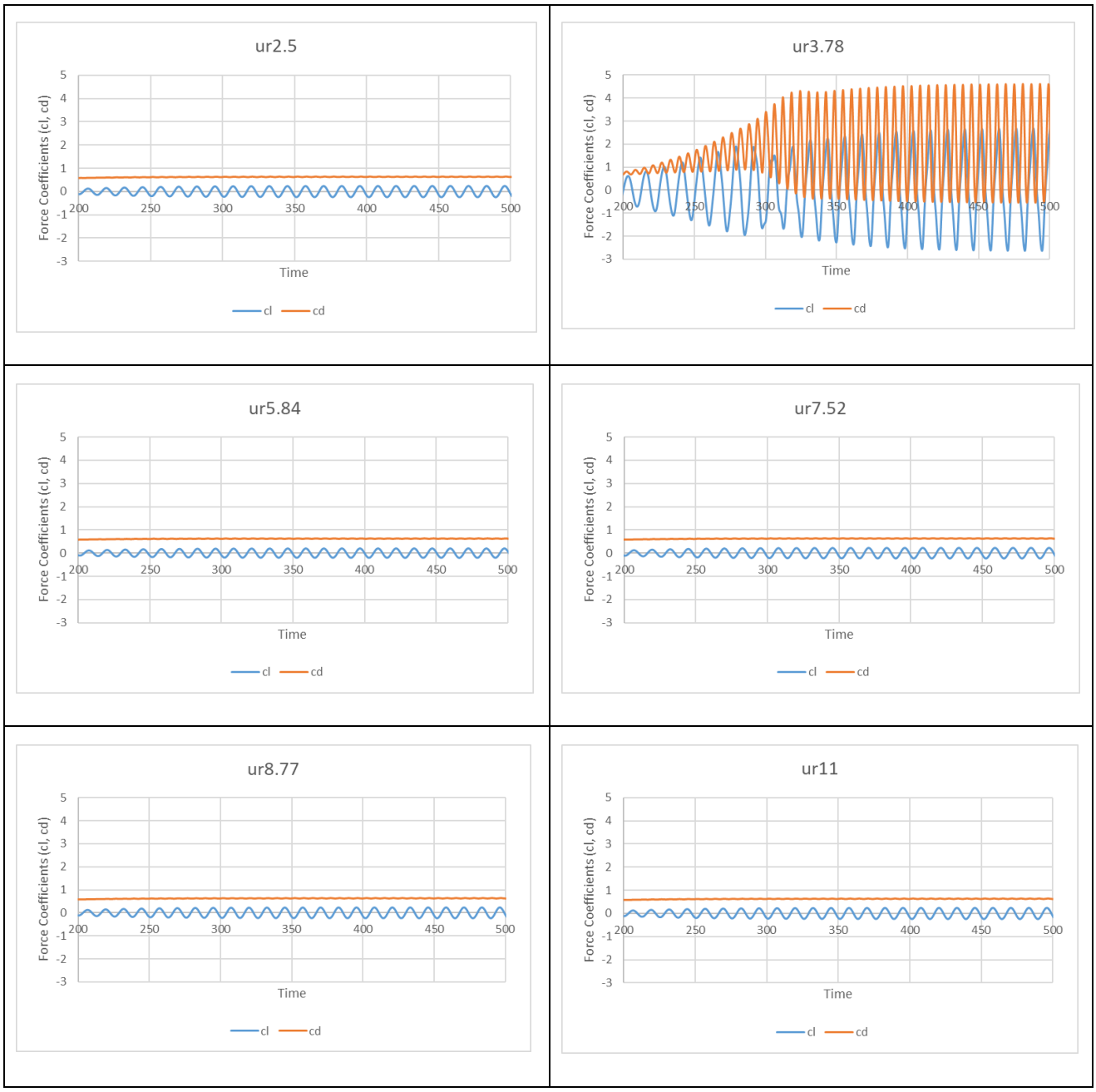

Figure 34. Time history of force coefficients (cd & cl) at (Ur=2.5, 3.78, 5.84, 7.52, 8.77 & 11)

Conclusion

The study was performed to investigate the impact of surface roughness on vortex shape, crossflow amplitude and lock-in region. The study was performed for a rough cylinder (i.e., Ks/ D=2×10−2) at mass ratio, m*=11. The results obtained from this study were compared with that of smooth cylinder. All the parameters in both cases for kept same. It was found that rough cylinder had a narrower lock-

in region and reduced amplitude response. As a result of surface roughness, the lock-in region was shifted towards low reduced velocities. 2P vortex mode was found at peak amplitude response at a low reduced velocity of Ur=3.78. At higher reduced velocities, low amplitude response was observed with the formation of 2S vortex mode in the wake. Lift forces & drag forces were found to be high in lock-in region & out of lock-in they were found to be low for rough cylinder at m*=11.

Chapter 5: Conclusion and future work

5.1 Conclusion

The study was performed for investigation of the VIV phenomenon, for an elastically mounted rigid cylinder free to oscillate in traverse direction direction at reduced velocities in the range of Ur = 2 to 14 with Reynolds number fixed at Re = 10^4. One of the objectives of the study was also to test the capability of 2d RANS approach and kw-SST model. The work concentrates on the impact of mass ratio and surface roughness on VIV phenomenon in a 2D circular cylinder having different mass ratios and surface roughness at a high Reynolds Number (Re) = 10^4.

For smooth cylinder with m*=11, it was found from the study that kw-SST was successful in capturing all three branch responses (Initial branch, Upper branch and lower branch) and it also successfully captured 2S & 2P vortex modes for the corresponding amplitude responses and their branches. However, peak amplitude responses were a little lower in comparison to the numerical (DES model) and experimental study which could be explained due to lower aspect ratio of mesh. But comparatively, the study was computationally less expensive and was also less time consuming, which concludes that 2D RANS approach and kw-SST turbulent model is quite reliable and capable for the resolution of complex fluid flow problems.

For smooth cylinder with m*=2.4, the results obtained were compared with results obtained at m*=11 and literature review. It was found that with decrease in mass ratio the lock-in region widened and there was a significant increase in the cylinder amplitude response. This behavior has been reported in literature in previous numerical and experimental studies. With decrease in mass ratio, vortex modes of P+S, 2P & 2T appeared at reduced velocities ranging from Ur = 2 to 14. These vortex modes correspond to high amplitude responses and their appearance in wake region at low mass ratios and high Reynolds number has been reported in literature.

To investigate the impact of surface roughness on vortex shape, crossflow amplitude and lock-in region, the study was performed for a rough cylinder (i.e., Ks/ D=2×10−2) at mass ratio, m*=2.4 and 11. The results obtained from this study were compared with that of smooth cylinder. It was found that rough cylinders had a narrower lock-in region and reduced amplitude response. As a result of surface roughness, the lock-in region was shifted towards low reduced velocities. For rough cylinder with m*=2.4, 2P & 2T vortex modes were found at low reduced velocities with high amplitude responses. Formation of these vortex modes have also been reported in literature for rough cylinder. At higher

reduced velocities, low amplitude response was observed with the formation of 2S vortex mode in the wake. It was observed lift forces decreased with increase in reduced velocity, drag forces were found to be high in lock-in region & low in out of lock-in region.

For rough cylinder with m*=11, 2P vortex mode was found at peak amplitude response at a low reduced velocity of Ur=3.78. At higher reduced velocities, low amplitude responses were observed with the formation of 2S vortex mode in the wake. Lift forces & drag forces were found to be high in lock-in region and out of lock-in they were found to be low.

5.2 Future work

In this project, we found that amplitude response of the cylinder was less compared to that of experimental studies and Numerical DES model. So, a different mesh configuration and tweaking the dynamic meshing parameters can result in better values. This study can be performed at transient formulation of First order, but transient formulation of 2^{nd} order would give more accurate results but it is considerably more computationally expensive as compared to the first order but it

This study was performed on very limited values of mass ratio and surface roughness. This study could be further expanded by utilizing a range of values for both mass ratio and surface roughness.

Appendix

User Defined Function (UDF File)

```
#include "udf.h"

DEFINE_SDOF_PROPERTIES(stage, prop,dt, time, dtime)
{
  real cg;
  real vel;
  real mass = 1884;
  real md = 785;
  real fn = 0.0833;
  real wn = 2*3.14*fn;
  real z = 0.001;
  real k = mass*wn*wn;
  real c = 2*mass*wn*z;

        prop[SDOF_MASS] = 1884;
        prop[SDOF_ZERO_TRANS_X] = TRUE;
        prop[SDOF_ZERO_TRANS_Z] = TRUE;

        prop[SDOF_ZERO_ROT_X] = TRUE;
        prop[SDOF_ZERO_ROT_Y] = TRUE;
        prop[SDOF_ZERO_ROT_Z] = TRUE;

        cg = DT_CG(dt)[1];
        vel = DT_VEL_CG(dt)[1];
        prop[SDOF_LOAD_F_Y] = -k*cg - vel*c;

        Message("\nNew Location = %g", DT_CG(dt)[1]);
        Message("\nNew Velocity = %g", DT_VEL_CG(dt)[1]);
        Message("\nNew Force = %g", -k*cg - vel*c);
        printf ("\nstage: updated 6DOF properties");
        }
```

References

[1] Feng, C. C., 1969. *The Measurement of Vortex Induced Effects in Flow Past Stationary and Oscillating Circular and D-Section Cylinders*, Vancouver: The University of British Columbia.

[2] Blevins RD. 2001. Flow-induced vibration. 2nd ed. Malabar, FL: Krieger Publishing, Inc.

[3] Breuer M. Large eddy simulation of the subcritical flow past a circular cylinder: numerical and modeling aspects. International Journal for Numerical Methods in Fluids. 1998; 28(9):1281–302.

[4] Sarpkaya T. A critical review of the intrinsic nature of vortex-induced vibrations. Journal of Fluids and Structures. 2004; 19(4):389–447.

[5] Bearman, P. W., 2011. Circular cylinder wakes and vortex-induced vibrations. *Journal of Fluids and Structures*, Volume 27, pp. 648-658.

[6] Placzek A, Sigrist J-F, Hamdouni A. Numerical simulation of an oscillating cylinder in a cross-flow at low Reynolds number: forced and free oscillations. Computers & Fluids. 2009; 38(1):80–100.

[7] Zhao M, Cheng L, An H, Lu L. Three-dimensional numerical simulation of vortex-induced vibration of an elastically mounted rigid circular cylinder in steady current. Journal of Fluids and Structures. 2014; 50:292–311.

[8] Khan NB, Jameel M, Badry ABBM, Ibrahim ZB, editors. Numerical Study of Flow Around a Smooth Circular Cylinder at Reynold Number = 3900 With Large Eddy Simulation Using CFD Code. ASME 2016 35th International Conference on Ocean, Offshore and Arctic Engineering; 2016: American Society of Mechanical Engineers.

[9] Khalak A, Williamson C. Dynamics of a hydroelastic cylinder with very low mass and damping. Journal of Fluids and Structures. 1996; 10(5):455–72.

[10] Guilmineau E, Queutey P. Numerical simulation of vortex-induced vibration of a circular cylinder with low mass-damping in a turbulent flow. Journal of fluids and structures. 2004; 19(4):449–66.

[11] Pan Z, Cui W, Miao Q. Numerical simulation of vortex-induced vibration of a circular cylinder at low mass-damping using RANS code. Journal of Fluids and Structures. 2007; 23(1):23–37.

[12] Li W, Li J, Liu S, editors. Numerical simulation of vortex-induced vibration of a circular cylinder at low mass and damping with different turbulent models. OCEANS 2014-TAIPEI; 2014: IEEE.

[13] Nguyen V-T, Nguyen HH. Detached eddy simulations of flow induced vibrations of circular cylinders at high Reynolds numbers. Journal of Fluids and Structures. 2016; 63:103–19.

[14] Hover F, Miller S, Triantafyllou M. Vortex-induced vibration of marine cables: experiments using force feedback. Journal of fluids and structures. 1997; 11(3):307–26.

[15] Khan NB, Ibrahim Z, Nguyen LTT, Javed MF, Jameel M (2017) Numerical investigation of the vortex-induced vibration of an elastically mounted circular cylinder at high Reynolds number (Re = 10^4) and low mass ratio using the RANS code. PLoS ONE 12(10): e0185832.

[16] Okajima A, Nagamori T, Matsunaga F, Kiwata T. 1999. Some experiments on flow-induced vibration of a circular cylinder with surface roughness. J Fluids Struct. 13:853–864.

[17] Allen DW, Henning DL. 2001. Surface roughness effects on vortex-induced vibration of cylindrical structures at critical and supercritical Reynolds numbers. Proceedings of the Offshore Technology Conference; 2001 Apr 30−May 3; Houston, Texas, USA.

[18] Bernitsas MM, Raghavan K, Duchene G. 2008. Induced separation and vorticity using roughness in VIV of circular cylinders at 8 × 103 < Re < 2.0 × 105. Proceedings of the Offshore Mechanics and Arctic Engineering Conference; 2008 June 15–20; Estoril, Portugal.

[19] Kiu KY, Stappenbelt B, Thiagarajan KP. 2011. Effects of uniform surface roughness on vortex-induced vibration of towed vertical cylinders. J Sound Vib. 330:4753−4763.

[20] Gao Y, Fu S,Wang J, Song L, Chen Y. 2015. Experimental study of the effects of surface roughness on the vortex-induced vibration response of a flexible cylinder. Ocean Eng. 103:40–54.

[21] Yun Gao, Zhi Zong, Li Zou & Zongyu Jiang (2018): Effect of surface roughness on vortex-induced vibration response of a circular cylinder, Ships and Offshore Structures, DOI: 10.1080/17445302.2017.1335577

[22] B Stappenbelt, F Lalji, G Tan (2007). Low mass ratio vortex-induced motion, 16th Australasian fluid mechanics conference 12, 1491-1497

[23] Alireza Modir, Mohsen Kahrom, Anoshirvan Farshidianfar. 2016. Mass ratio effect on vortex induced vibration of a flexibly mounted circular cylinder, an experimental study, International Journal of Marine Energy.

[24] Menter FR. Two-equation eddy-viscosity turbulence models for engineering applications. AIAA journal. 1994; 32(8):1598–605.

[25] Shao J, Zhang C. Numerical analysis of the flow around a circular cylinder using RANS and LES. International Journal of Computational Fluid Dynamics. 2006; 20(5):301–7.

[26] Fang YY, Han ZL, editors. Numerical experimental research on the hydrodynamic performance of flow around a three-dimensional circular cylinder. Applied Mechanics and Materials; 2011: Trans Tech Publ.

[27] Franke J, Frank W. Large eddy simulation of the flow past a circular cylinder at Re D = 3900. Journal of wind engineering and industrial aerodynamics. 2002; 90(10):1191–206.

[28] Zdravkovich M. Conceptual overview of laminar and turbulent flows past smooth and rough circular cylinders. Journal of wind engineering and industrial aerodynamics. 1990; 33(1–2):53–62.

[29] Navrose, MS. 2013. Free vibrations of a cylinder: 3-D computations at Re = 1000. J Fluids Struct. 41:109–118.

[30] Zhao M, Tong F, Cheng L. 2012. Numerical simulation of twodegree-of-freedom vortex-induced vibration of a circular cylinder between two lateral plane walls in steady currents. J Fluids Eng. 134:104501

[31] ANSYS 2016. Ansys fluent manual r, ANSYS, Inc.

[32] Williamson, C.H.K., Govardhan, R., 2004. Vortex-induced vibrations. Annu. Rev. Fluid Mech. 36 (1), 413–455.

[33] NAS Ramzi, L K Quen, 2019. Experimental analysis on vortex-induced vibration of a rigid cylinder with different surface roughness, IOP Conference Series: Materials Science and Engineering, Volume 469.

[34] Mohd Ghazali, M. K. ., Shaharuddin, N. M. R. ., Ali, A. ., Siang, K. H. ., Mohd Nasir, M. N. ., & Ab. Talib, M. H. . (2020). Surface Roughness Effect on Vortex-Induced Vibration Phenomenon in Cross-Flow Direction of a Bluff Body. Journal of Advanced Research in Fluid Mechanics and Thermal Sciences, 64(2),

[35] Yun Gao, Z Zhang, L Zou, L Liu, B Yang. 2020. Effect of surface roughness and initial gap on the vortex-induced vibrations of a freely vibrating cylinder in the vicinity of a plane wall, Marine Structures.

[36] Xiangxi Han, Youhong Tang, Zhanbin Meng, Fei Fu, Ang Qiu, Jian Gu, Jiaming Wu, 2021. Surface roughness effect on cylinder vortex-induced vibration at moderate Re regimes, Ocean Engineering, Volume 224.

[37] Jisheng Zhao, Justin Leontini, David Lo Jacono, John Sheridan, 2019. The effect of mass ratio on the structural response of a freely vibrating square cylinder oriented at different angles of attack, Journal of Fluids and Structures, Volume 86, Pages 200-212.

[38] Pigazzini, R., Contento, G., Martini, S. et al. An investigation on VIV of a single 2D elastically-mounted cylinder with different mass ratios. J Mar Sci Technol 24, 1078–1091 (2019).

[39] M.H. Bahmani, M.H. Akbari, 2010. Effects of mass and damping ratios on VIV of a circular cylinder, Ocean Engineering,Volume 37, Issues 5–6, Pages 511-519.

[40] Zhaolie Tang, Benmou Zhou, 2020. The effect of mass ratio and spring stiffness on flow-induced vibration of a square cylinder at different incidence angles, Ocean Engineering, Volume 198.

[41] Dongyang Chen, Pier Marzocca, Qing Xiao, Zhihuan Zhan, Chaojie Gu, 2020. Vortex-induced vibration on a low mass ratio cylinder with a nonlinear dissipative oscillator at moderate Reynolds number, Journal of Fluids and Structures, Volume 99.

[42] Bishop R, Hassan A, editors. The lift and drag forces on a circular cylinder oscillating in a flowing fluid. Proceedings of the Royal Society of London A: Mathematical, Physical and Engineering Sciences; 1964: The Royal Society.